Coupling between quantum dot excitons and microcavity photons

Diplomarbeit

zur Erlangung des akademischen Grades einer
Magistra der Naturwissenschaften

am Institut für Physik, FB Theoretische Physik
der Karl-Franzens Universität Graz

vorgelegt von
Gabriele JARITZ

Betreuer: Ao. Univ. Prof. Mag. Dr. Ulrich Hohenester

Graz, Juli 2009

Contents

Kurzfassung / Abstract

Kopplung von Quantenpunkt-Exzitonen mit Mikrokavitäts-Photonen

In dieser Arbeit wird die Kopplung eines Quantenpunkt an eine Mikrokavität im Bereich starker Kopplung untersucht. Die Beschreibung dieses offenen Quantensystems erfolgt über den Dichtematrixformalismus und die Lindbladgleichung. Ein kontrollierter Transfer der Population der elektronischen Zustände wird über einen modifizierten STIRAP Prozess erreicht. Die Reaktion des Systems auf Verstimmungen des Lasers und der Kavitätsmode gegenüber den elektronischen Übergängen wird untersucht. Als Teil dieses Prozesses wird ein Photon mit bestimmter Polarisationsrichtung aus der Kavität emittiert. Eine Aufspaltung der energetischen Zustände des Quantenpunktes und die Existenz zweier Kavitätsmoden ermöglichen die Herstellung von verschränkten Photonen.

Coupling between quantum dot excitons and microcavity photons

In this work we investigate the coupling of a quantum dot with a microcavity in the strong coupling regime. This open quantum system is described with the density matrix formalism and the Lindblad master equation. We use a modified STIRAP process to transfer the population of the electronic states in a controlled way. The behavior of the system under detunings of the driving field and the cavity mode are investigated. During the STIRAP process a cavity photon of well defined polarization is emitted. A cavity sustaining two modes and a splitting of the energy levels of the quantum dot, offers the possibility to theoretically produce entangled photonic states.

Chapter 1

Quantum dots and micro-cavities

In this work we study the interaction of an artificial atom (quantum dot) with a single mode of the electromagnetic field in a cavity. Such studies belong to the field of *Cavity quantum electrodynamics* (CQED).
To start with, we give a short introduction to the physical properties of quantum dots and cavities, and how they are produced.

1.1 Quantum dots

Quantum dots (QDs) are often referred to as "artificial atoms", because of their atom-like, discrete energy levels. This is why QDs emit light of a discrete spectrum. QDs are mostly made out of semiconductors, exploiting the different band gap energies of the materials. Figure 1.1 shows a simplified model of the energy levels and band gap energies of a QD consisting of InAs embedded in GaAs.
There are different ways to produce a QD. They can be realized by [4]:

1. Deep-mesa-etched dots
2. Field effect confined dots
3. Self-assembled dots.

The first method starts with a sample of modulation-doped AlGaAs/GaAs heterostructures. Deep-mesa-etched dots can be fabricated using a mask of photo resistant dots. Then, deep grooves of about 200 nm are etched into the material.

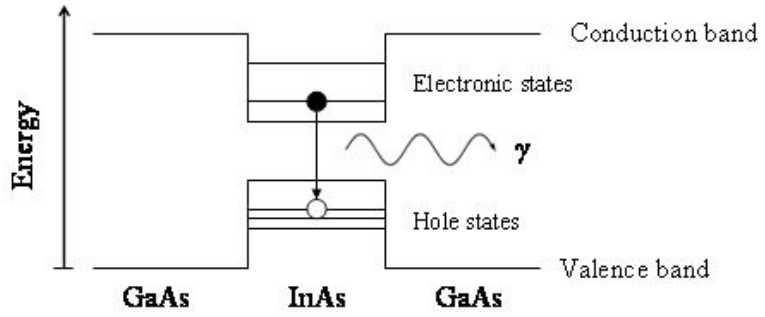

Figure 1.1: Simplified band gap scheme of an InAs QD. The effective potential of the QD shows discrete energy levels.

Field effect confined quantum dots are prepared starting with a 2D electron gas, e.g. in the interface between n-AlGaAs and GaAs. Confinement in the other two dimensions is reached by applying a gate voltage.
Self-assembled quantum dots use the different lattice constants of different semiconductors. This idea is explained in the next section.

1.1.1 Producing self-assembled QDs

[1] Producing self-assembled QDs, the lattice mismatch between GaAs and InAs is used. The process starts with a flat GaAs surface. Then, via epitaxial growth, a layer of InAs is formed at the surface. The lattice constant of InAs is about 7% larger than that of GaAs. After more than 1.75 monolayers the strain destroys the flat surface and small islands of InAs are formed. In the last step, the islands are covered with a GaAs layer. Now they form QDs. The arrangement of the quantum dots is random. Figure 1.2 shows the procedure. An ordinary QD is about $3-4$ nm high and the basis is about $10-25$ nm in diameter [8].

1.2 Optical microcavities

Optical microcavities offer a way to confine light to very small volumes. Optical mirrors are used to trap the light by resonant forth- and backscattering between

[1] This section is mainly based on the article of Stumpf [14].

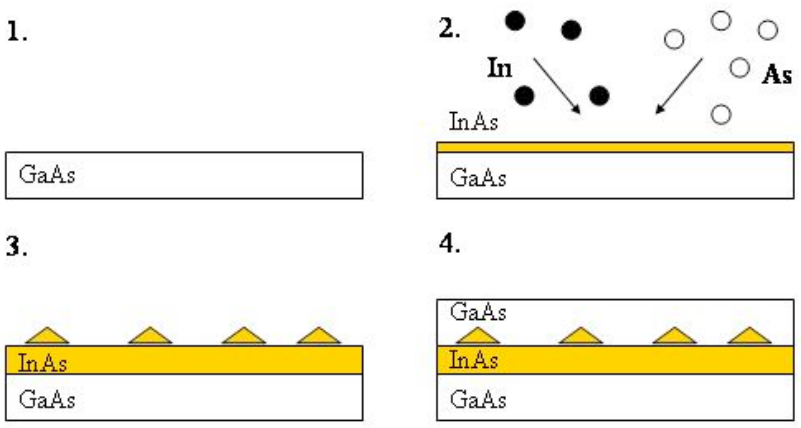

Figure 1.2: The four steps, producing self-assembled Indiumarsenide quantum-dots embedded in a Galliumarsenide crystal.

the mirrors. In reality, these mirrors are not perfect, resulting in a photon loss after a finite time. The dimensionless quality factor Q, which is proportional to the average lifetime of the resonant photon in the cavity, gives information about the quality of the cavity. The other relevant factor is the volume V of the cavity. The smaller the volume of the cavity is, the higher is the field intensity at a specific point (antinode) inside the cavity. There are many applications based on optical microcavities and also a lot of different ways to realize one. Common microcavity designs are:

1. Micropillar

2. Microdisc

3. Photonic crystal slab

The micropillar cavity emits light in the vertical direction, which makes optical access to it easy. The emission direction from a microdisc is not as well defined. Its advantage is a high Q-factor for some modes. The photonic crystal slab nanocavity has a very small volume. Depending on its design, the emitted light occurs in the plane or perpendicular to the plane. For further reading see Refs. [8] and [15].

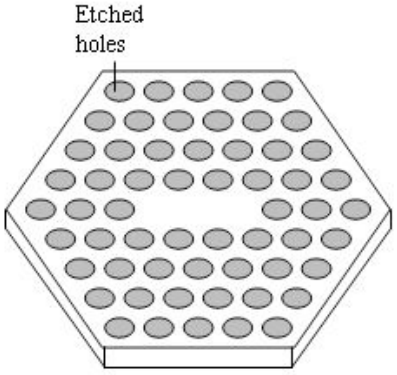

Figure 1.3: The photonic crystal nanocavity confines the light creating a 'defect' in the hole-array.

1.2.1 Photonic crystal slab microcavities

A photonic crystal uses the reflection and scattering properties of electromagnetic waves in periodic materials (Bragg reflection). The simplest case of a one-dimensional photonic crystal consists of alternating layers with different dielectric constants. If the wave length of the light is of the same order as the periodicity of the crystal, the reflected waves interfere. This results in a photonic band structure. Big differences in the dielectric constants of the layers can generate a photonic band gap. Light at a frequency within the band gap is not able to propagate. Such a periodic structure works like a perfect mirror. The band gap depends on the angle, because the periodicity of the crystal depends on the direction [7, 15, 14].

A photonic crystal slab nanocavity consists of a photonic crystal with point-defects in the periodic structure. These defects have the effect of a little resonator which confines the light. This can be realized for instance using a thin dielectric membrane, with hexagonal ordered holes on it. The defects are areas where the hole is missing. This is illustrated in figure 1.3. Such small structures can be realized via electron beam lithography combined with etching techniques [14].
Because of the nanoscopic scale of these defects, the light can be confined in very small volumes. In analogy to the discrete energy levels in quantum dots, also

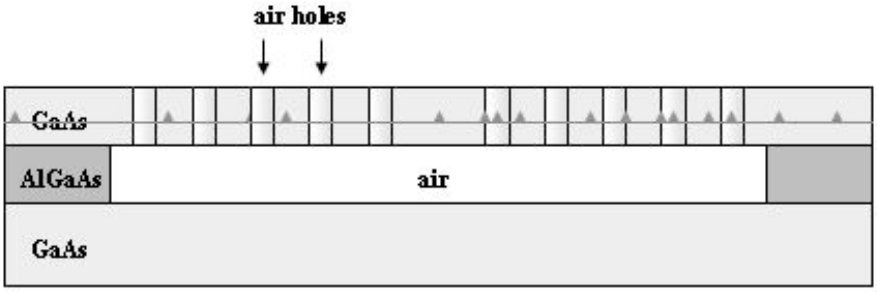

Figure 1.4: A two dimensional photonic crystal nanocavity containing self assembled InAs quantum dots.

in a nano-resonator only discrete energies are allowed. Therefore, the optical modes are quantized.

1.3 Realization of a CQED system

One method to realize a system consisting of an artificial atom within a cavity is the combination of self-assembled quantum dots and a photonic crystal slab cavity. Therefore, a heterostructure consisting of a GaAs membrane, followed by an AlGaAs layer and a GaAs layer containing self-assembled InAs quantum dots. The quantum dots are produced as described in section (1.1.1). Now the technique explained in section (1.2.1) is used, to produce a nano-resonator. Figure 1.4 shows the idea.

Atomic force microscopy (AFM) offers a way to locate the position of buried quantum dots. This makes it possible to position the nanocavity with 30 nm accuracy to one quantum dot, arranging it to the electric-field maximum [6].

Chapter 2

Closed and open quantum systems

The dynamic of closed systems can be represented in terms of a unitary time evolution. The central equation is the Liouville- von Neumann equation[1], which is a differential equation for the density matrix. In contrast, the time evolution of an open quantum system is not unitary. For Markovian dynamics, an appropriate equation of motion is given by a first-order linear differential equation for the reduced density matrix. It is known as quantum master equation in Lindblad form. We start with the important concept of the density operator. Then, the dynamic of a closed system is described respectively in the Schrödinger-, Heisenberg-, and interaction picture. Finally the dynamic of an open system and the Lindblad master equation are briefly discussed.

2.1 The density operator

The density operator is a generalization of the wave function, including uncertainties about the state of the system. If the system is described by an ensemble of states $\{|\psi_n\rangle\}$, in which it may reside with probabilities $\{p_n\}$, the density op-

[1] Obviously, the Liouville- von Neumann equation holds also for the combined density matrix $\hat{\rho}$ of an open system, since the combination of an open system and its environment is closed.

erator is

$$\hat{\rho}(t) = \sum_n p_n |\psi_n(t)\rangle\langle\psi_n(t)|. \tag{2.1}$$

The density matrix gets important in the description of open quantum systems. But it has also relevance for closed systems, when the system under consideration is in a mixed state. The diagonal elements tell us about the probability to find the system in the corresponding state, which is often referred to as *population*. The off-diagonal elements give information about the *coherence* between the respective states.
Note that the terms 'density matrix' and 'density operator' are used interchangeably here.

Properties of $\hat{\rho}$:

1. Positivity condition: $\hat{\rho}$ is a positive operator. The eigenvalues of the density matrix take real and non-negative values.
   They give the probabilities of finding the system in the corresponding eigenstate.

2. Trace condition: $\hat{\rho}$ has trace equal to one,

   $$\mathrm{tr}\hat{\rho} = 1. \tag{2.2}$$

   This restriction follows from probability conservation.

3. The density matrix is hermitian

   $$\hat{\rho}^\dagger = \hat{\rho}. \tag{2.3}$$

4. The density operator characterizes the quantum state as follows:

   - If $\mathrm{tr}\hat{\rho}^2 = \mathrm{tr}\hat{\rho} = 1$ the quantum state is pure.
   - If $\mathrm{tr}\hat{\rho}^2 < \mathrm{tr}\hat{\rho} = 1$ the quantum state is mixed.

5. The expectation value of any operator can be calculated from $\hat{\rho}$ according to

$$\left\langle \hat{O} \right\rangle = \mathrm{tr}\left[\hat{O}\hat{\rho}\right]. \tag{2.4}$$

2.2 Closed systems

Closed systems are described by a single wave function ψ. The time evolution is given by the Schrödinger equation

$$\partial_t |\psi(t)\rangle = -\frac{i}{\hbar}\hat{H}(t)|\psi(t)\rangle. \tag{2.5}$$

$\hat{H}$ is the Hamiltonian of the system. The solution of this equation defines the time evolution operator. It acts on the state vector ψ, and transforms it from some initial time t_0 to some later time t,

$$|\psi(t)\rangle = \hat{U}(t, t_0)|\psi(t_0)\rangle. \tag{2.6}$$

The resulting time evolution operator U is unitary

$$\hat{U}^\dagger \hat{U} = \hat{U}\hat{U}^\dagger = \hat{1}, \tag{2.7}$$

since the norm of the state vector is conserved. In the case of a time-independent Hamiltonian, the time evolution operator takes the form

$$\hat{U}(t, t_0) = \exp\left[-\frac{i}{\hbar}\hat{H}(t - t_0)\right]. \tag{2.8}$$

If the system is driven by an external field, the Hamiltonian gets time dependent and the time-evolution operator may be written as the time ordered exponential,

$$\hat{U}(t, t_0) = \hat{T}\exp\left[-\frac{i}{\hbar}\int_{t_0}^{t} dt' \hat{H}(t')\right]. \tag{2.9}$$

$\hat{T}$ denotes the time ordering operator, which orders the operators from the right to the left with increasing time.

If the system is in a mixed state, the description via the density operator $\hat{\rho}$ is adequate. The time dependence of the density operator in a closed system is obtained by taking the time derivative of the bra and ket in equation (2.1), and using equation (2.5)

$$\begin{aligned}\frac{d}{dt}\hat{\rho} &= \sum_n p_n \left[(\partial_t |\psi_n(t)\rangle) \langle\psi_n(t)| + |\psi_n(t)\rangle (\partial_t \langle\psi_n(t)|) \right] \\ &= \frac{1}{i\hbar} \sum_n p_n \hat{H}(t) |\psi_n(t)\rangle\langle\psi_n(t)| - \frac{1}{i\hbar} \sum_n p_n |\psi_n(t)\rangle\langle\psi_n(t)| \hat{H}(t) \\ &= -\frac{i}{\hbar} \left[\hat{H}(t), \hat{\rho}(t) \right]. \end{aligned} \tag{2.10}$$

This is often referred to as the *Liouville- von Neumann equation.*
The solution to this equation may be written

$$\hat{\rho}(t) = \hat{U}(t, t_0) \hat{\rho}(t_0) \hat{U}^\dagger(t, t_0). \tag{2.11}$$

2.2.1 The Heisenberg picture

In the Schrödinger picture, the time dependence is carried by the state vector, and can be described by an equation of motion for the density matrix (2.10). But this is not the only valid description of quantum mechanics. In the Heisenberg picture, time dependence is transferred to the operators and the state vector is time independent. At some initial time t_0 we assume the operators and states to be the same in both pictures. The index H indicates the Heisenberg picture. The descriptions are physically equivalent, and the expectation value of an observable should be the same in both pictures,

$$\langle \hat{O}(t) \rangle = \mathrm{tr} \left[\hat{O}(t) \hat{\rho}(t) \right] = \mathrm{tr} \left[\hat{O}_H(t) \hat{\rho}_H(t_0) \right]. \tag{2.12}$$

Here, the Schrödinger picture operator is allowed to be explicitly time dependent.
Since the trace is invariant under cyclic permutations and $\rho(t)$ is given by equation (2.11), we find that the operators are related through a canonical transformation,

$$\hat{O}_H(t) = \hat{U}^\dagger(t, t_0) \hat{O}(t) \hat{U}(t, t_0). \tag{2.13}$$

We arrive at the equation of motion for a Heisenberg operator, when differentiating both sides of equation (2.13),

$$\frac{d}{dt}\hat{O}_H(t) = \frac{i}{\hbar}\left[\hat{H}_H(t), \hat{O}_H(t)\right] + \frac{\partial \hat{O}_H(t)}{\partial t}. \tag{2.14}$$

$\hat{H}_H(t)$ is the Hamiltonian in the Heisenberg picture. The second term, the partial derivative, gets important, if the Schrödinger-picture-operator $\hat{O}$ is explicitly time dependent. It is given by

$$\frac{\partial \hat{O}_H(t)}{\partial t} = \hat{U}^\dagger(t, t_0)\frac{\partial \hat{O}(t)}{\partial t}\hat{U}(t, t_0). \tag{2.15}$$

This term cancels, if the operator is not explicitly time dependent.
If the Hamiltonian in the Schrödinger picture has no time dependence, we call the system isolated. In this case, the time evolution operator takes the form (2.8). Since this expression commutes with the Hamiltonian, we get $\hat{H}_H(t) = \hat{H}$. It follows, that the Heisenberg picture Hamiltonian is a constant of motion, which means $d\hat{H}_H/dt = 0$.
If the system is isolated and the operator $\hat{O}$ is not explicitly time dependent, the Heisenberg equation of motion reads,

$$\frac{d}{dt}\hat{O}_H(t) = \frac{i}{\hbar}\left[\hat{H}, \hat{O}_H(t)\right]. \tag{2.16}$$

2.2.2 The interaction picture

In the interaction picture, both the states and the operators are time dependent. The Hamiltonian of the system is written as the sum of a free part, which is time-independent, and an interaction part,

$$\hat{H}(t) = \hat{H}_0 + \hat{H}_1(t). \tag{2.17}$$

As mentioned, the equivalence of the expectation value ensures the physical equivalence of the two pictures. Therefore, our starting point is again the expectation value of an arbitrary Schrödinger operator $\hat{O}$,

$$\langle \hat{O}(t) \rangle = \mathrm{tr}\left[\hat{O}(t)\hat{\rho}(t)\right] = \mathrm{tr}\left[\hat{O}(t)\hat{U}(t, t_0)\hat{\rho}(t_0)\hat{U}^\dagger(t, t_0)\right]. \tag{2.18}$$

Defining the time evolution operators

$$\hat{U}_0(t,t_0) \equiv \exp[-\frac{i}{\hbar}\hat{H}_0(t-t_0)], \quad \hat{U}_I(t,t_0) \equiv \hat{U}_0^\dagger(t,t_0)\hat{U}(t,t_0), \tag{2.19}$$

equation (2.18) can be written in the form,

$$\begin{aligned} \langle\hat{O}(t)\rangle &= \mathrm{tr}\left[\hat{U}_0^\dagger(t,t_0)\hat{O}(t)\hat{U}_0(t,t_0)\hat{U}_I(t,t_0)\hat{\rho}(t_0)\hat{U}_I^\dagger(t,t_0)\right] &(2.20)\\ &= \mathrm{tr}\left[\hat{O}_I(t)\hat{\rho}_I(t)\right]. &(2.21)\end{aligned}$$

The second equality sign follows by introducing the interaction picture operator

$$\hat{O}_I(t) = \hat{U}_0^\dagger(t,t_0)\hat{O}(t)\hat{U}_0(t,t_0), \tag{2.22}$$

and the interaction picture density matrix

$$\hat{\rho}_I(t) = \hat{U}_I(t,t_0)\hat{\rho}(t_0)\hat{U}_I^\dagger(t,t_0). \tag{2.23}$$

The corresponding equation of motion for the density matrix in the interaction picture is obtained by differentiating both sides of equation (2.23)

$$\frac{d}{dt}\rho_I(t) = -\frac{i}{\hbar}\left[\hat{H}_I(t), \hat{\rho}_I(t)\right]. \tag{2.24}$$

This is the von Neumann equation in the interaction picture.
The equation of motion for the operators results in

$$\frac{d}{dt}\hat{O}_I(t) = \frac{i}{\hbar}\left[\hat{H}_0(t), \hat{O}_I(t)\right] + \frac{\partial}{\partial t}\hat{O}_I(t). \tag{2.25}$$

Again, the partial derivative cancels if the the Schrödinger-picture-operator $\hat{O}$ is not explicitly time dependent.
In the interaction picture, the time dependence is shared between operators and states. The free part of the Hamiltonian determines the time evolution of the operators. The states move because of the interaction.

2.3 Open systems

[2] In the real world, there are no perfectly closed systems. An exception is perhaps the universe as a whole. Open systems are influenced by uncontrolled interactions with the environment. In quantum information processing systems these interactions show up as noise. The time evolution of an open system is not unitary anymore and the description with a single wave function not adequate. The more generalized construct, the density operator, offers an alternative to describe open quantum systems.
An open system can be viewed as a quantum system S, coupled to an other quantum system E called the environment. The whole system $S+E$ is assumed to be closed, and therefore follows Hamiltonian dynamics. The subsystem S, which is called the reduced system, is driven by some internal dynamics, but it is also influenced by the interaction with the environment. Because of these interactions, the reduced system can not be described by unitary dynamics. When dealing with open quantum systems, the density matrix of the reduced system is of interest. It is obtained by tracing over the degrees of freedom of the environment,

$$\hat{\rho}_S = \mathrm{tr}_\mathrm{E}\hat{\rho}. \tag{2.26}$$

ρ determines the density matrix of the combined system. The expectation value of an observable acting on the open quantum system S is given by

$$\langle\hat{O}\rangle = \mathrm{tr}_\mathrm{S}\left[\hat{O}\hat{\rho}_S\right]. \tag{2.27}$$

The reason for studying open quantum systems is that a complete mathematical description of the complete system is much too complicated. The environment often consists of many degrees of freedom. In the case of a heat bath, this number is even infinity. Sometimes, the modes of the environment are not even known exactly. But even if we could handle this, we would not be interested in these irrelevant degrees of freedom. We therefore describe the system via a reduced set of variables and the *reduced density matrix*.

[2] A useful text on open quantum systems can be found at: http://cmmp.ucl.ac.uk/~ajf/course_notes.pdf

2.3.1 The Lindblad master equation

The Lindblad master equation is an equation of motion for the reduced density matrix. It describes the dynamics of an open quantum system. In order to arrive at the equation of motion we use the theory of quantum operations. During the derivation, we look at the dynamics happening at a timescale δt that has to satisfy two conditions:

- $\delta t \ll \tau_{\mathrm{S}}$
  The time interval δt has to be much smaller than the characteristic timescale of the system τ_{S}. Therefore, the system density matrix can be considered to be constant during the time δt. Hence, the system density matrix can be handled as a continuous function in time.

- $\delta t \gg \tau_{\mathrm{E}}$
  The time δt should be long compared with the time which is necessary for the environment to forget its knowledge about the system. This is called the **Markovian limit** [**3**]. Because of this assumption we can hope that the time evolution of the system depends only on the actual density matrix and is not influenced by something that has happened in the past.

In the Markovian limit, the evolution can be described by a **quantum operation** or **super-operator** which acts on the present density matrix.
A quantum operation acts on density operators, not on states. It is completely positive and preserves the normalization of the state (trace preserving). Complete positivity is explained in appendix A.
With these assumptions, the time dependence of the density matrix of an open quantum system in the limit $\delta t \to 0$, is described by the **Lindblad master equation** [9]

$$\frac{d\hat{\rho}_S}{dt} = \frac{1}{i\hbar}\left[\hat{H}, \hat{\rho}_S\right] + \sum_k \left[\hat{L}_k \hat{\rho}_S(0) \hat{L}_k^\dagger - \frac{1}{2}\left\{\hat{\rho}_S(0), \hat{L}_k^\dagger \hat{L}_k\right\}\right]. \tag{2.28}$$

The L_k are the Lindblad operators and represent the influence of the interaction of the system with the environment. They describe all possible channels through which information can get outside the system. $\hat{H}$ is the system Hamiltonian, representing the coherent part of the dynamics.
Note that this equation gives us the time dependence of the reduced density

matrix $\hat{\rho}_S$. The Lindblad master equation is the most general description of non-unitary time evolution, that is trace preserving, completely positive and Markovian.

Chapter 3

Cavity QED

3.1 Dynamics of a quantum dot - cavity system

We consider a system of a quantum dot coupled to a cavity. The quantum dot is represented by an electronic two level system, the cavity by a single radiation-field mode. Because of coupling, the occupation can channel between these two states. We study the regime of strong coupling, where Rabi oscillations appear. In reality such systems are not perfect, meaning that a photon can get lost to the environment via scattering channels. We take two channels into account: The leaky cavity and the spontaneous emission of the quantum dot. The ratio of coupling strength to scattering rates defines the regime of strong/weak coupling.
Due to this 'imperfections' our system has to be treated as an open quantum system. Open systems are described by a density matrix ρ. The time dependence of ρ can be described by the Lindblad master equation, which was introduced in the previous chapter.

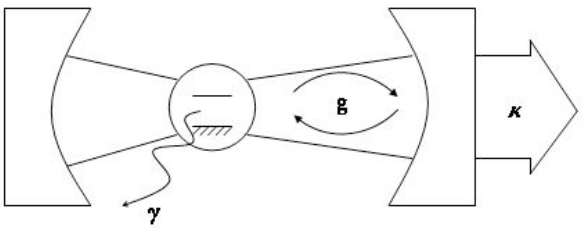

Figure 3.1: Scheme of a two level (artificial) atom coupled to a cavity. γ and κ are the scattering rates, and g is the coupling strength.

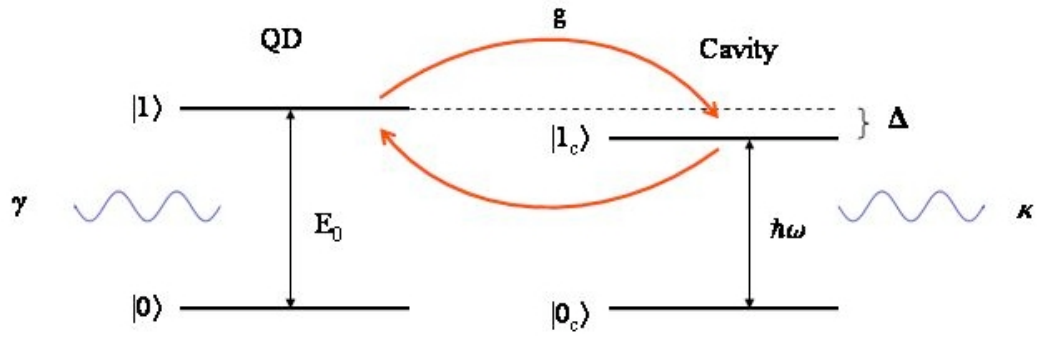

Figure 3.2: The energy levels of the QD-cavity system.

3.1.1 Formulation of the system

The fundamental theoretical tool in the study of cavity QED is the Jaynes-Cummings Hamiltonian [9]

$$\hat{H} = \hbar\omega a^\dagger a + E_0|1\rangle\langle 1| + \hbar g(\sigma_+ a + \sigma_- a^\dagger). \tag{3.1}$$

It describes the interaction between a two level atom (or artificial atom) and an electromagnetic field in the dipole- and rotating wave approximations [9, 17, 12]. a, $a^\dagger$ are the creation and annihilation operators of the photonic field, and $\sigma_+ = |1\rangle\langle 0|$, $\sigma_- = |0\rangle\langle 1|$ the electronic raising and lowering operators. σ_+ brings the electronic system from the ground state $|0\rangle$ to the excited state $|1\rangle$, and σ_- induces the transition from the excited state to the ground state.

The dipole approximation assumes that the wavelength of the electromagnetic field is much larger than the dimensions of the quantum emitter.
The rotating wave approximation neglects terms rotating at a very high frequency. This is equivalent to dropping the energy non conserving terms $(\sigma_+ a^\dagger, \sigma_- a)$ in the interaction part of the Hamiltonian $\hat{H}_I = \hbar g(\sigma_+ - \sigma_-)(a - a^\dagger)$.
This is a pretty good approximation here. A detailed explanation of the rotating wave approximation is given in appendix B.

The Hilbert space of the system is a direct product of the material part, which we associate here with a quantum dot (qd), and the photonic part, given by the

cavity mode (c):

$$\mathcal{H} = \mathcal{H}_{qd} \otimes \mathcal{H}_c. \tag{3.2}$$

If $\{|i\rangle_{qd}\}$ is a basis set for the electronic system and $\{|j\rangle_c\}$ is a basis set for the photonic system, then a basis set for the combined system is

$$\{|i,j\rangle\} = \{|i\rangle_{qd}|j\rangle_c\}. \tag{3.3}$$

First of all we want to study the occupation of the different states as a function of time. Occupation is given by the diagonal elements of the density matrix. So, we have to find a solution for $\hat{\rho}(t)$. The dynamics of the system is described by the Lindblad equation (2.28)
As will be shown below, there exists an analytic solution to this problem, which is based on the eigensystem of the effective Hamiltonian $\hat{H}_{\text{eff}}$. The basis we are working in is

$$\{|1,0\rangle, |0,1\rangle, |0,0\rangle\},$$

which states that the excitation is either in the electronic or in the photonic subsystem, or the system is in the ground state, corresponding to the situation where a photon has been emitted. In the end we are not interested in the vacuum state, and thus drop it. This is possible here, because we don't consider re-excitation from the ground state in our calculations. The basis reduces to:

$$\{|1,0\rangle, |0,1\rangle\},$$

As a consequence, the time evolution is not unitary anymore and $\text{tr}\hat{\rho} < 1$.
The two Lindblad operators take the form:

$$\hat{L}_1 = \sqrt{\gamma}\sigma_- \tag{3.4}$$
$$\hat{L}_2 = \sqrt{\kappa}a \tag{3.5}$$

3.1.2 The effective Hamiltonian

It can be easily seen that the last term in the Lindblad equation (2.28) only contributes to transitions to the vacuum. That means, in our two-dimensional

consideration, that we can drop this term and the Lindblad equation becomes[1]

$$\frac{d\hat{\rho}}{dt} = -i\left(\hat{H}_{\text{eff}}\hat{\rho} - \hat{\rho}\hat{H}_{\text{eff}}^{\dagger}\right), \tag{3.6}$$

where the effective Hamiltonian takes the form

$$\hat{H}_{\text{eff}} = \hat{H} - \frac{i}{2}\sum_i \hat{L}_i^{\dagger}\hat{L}_i. \tag{3.7}$$

In the interaction picture the Hamiltonian (3.1) takes the form

$$\hat{H}_I = \Delta|1\rangle\langle 1| + g\left(\sigma_+ a + \sigma_- a^{\dagger}\right), \tag{3.8}$$

where $\Delta = E_0 - \omega_c$ is the energy mismatch between quantum dot and cavity mode.
The effective Hamiltonian in the interaction picture reads

$$\hat{H}_{\text{eff}} = \Delta|1\rangle\langle 1| + g\left(\sigma_+ a + \sigma_- a^{\dagger}\right) - \frac{i}{2}\left(\gamma\sigma_+\sigma_- + \kappa a^{\dagger}a\right), \tag{3.9}$$

which in the two dimensional basis becomes

$$\hat{H}_{\text{eff}} = \begin{pmatrix} \Delta - \frac{i}{2}\gamma & g \\ g & -\frac{i}{2}\kappa \end{pmatrix}. \tag{3.10}$$

Left and right eigenvectors

As mentioned, our calculation is based on the eigensystem of the effective Hamiltonian. The usual method to obtain the eigensystem fails here, because our matrix is not normal. That means, that the matrix does not commute with its complex conjugate: $[\hat{H}_{\text{eff}}, \hat{H}_{\text{eff}}^{\dagger}] \neq 0$. As a consequence, the eigenvectors are not complete - they do not span the complete vector space. We denote the matrix defective.
However, it is possible to define right and left eigenvectors, where the left and

[1]Here $\hat{\rho}$ denotes the reduced density matrix of the system. For simplicity we set $\hbar = 1$.

right eigenvalues are identical [11]:

$$\hat{H}_{\text{eff}} X = X\Lambda \tag{3.11}$$

$$\tilde{X}\hat{H}_{\text{eff}} = \Lambda\tilde{X}. \tag{3.12}$$

Λ is the matrix of the eigenvalues, X and $\tilde{X}$ are the matrices of the right and left eigenvectors. For the case of non degenerate eigenvalues, the eigensystem of right and left eigenvectors is complete. By choice of normalization, the product of left and right eigenvectors can always be made unity

$$X\tilde{X} = \tilde{X}X = I. \tag{3.13}$$

3.1.3 Solution of $\hat{\rho}(t)$

The time dependence of the density matrix can be calculated now easily. The density matrix can be written as the outer product of the wave function

$$\hat{\rho}(t) = |\psi(t)\rangle\langle\psi(t)|. \tag{3.14}$$

The time dependence of the wave function is

$$|\psi(t)\rangle = \hat{U}(t,0)|\psi(0)\rangle \tag{3.15}$$

$$= \exp\left[-i\hat{H}_{\text{eff}}t\right]|\psi(0)\rangle \tag{3.16}$$

When multiplying the last equation from the left with $\tilde{X}$, applying equation (3.12) and again multiplying from the left with X, we arrive at

$$\hat{\rho}(t) = Xe^{-i\Lambda t}\tilde{X}|\psi(0)\rangle\langle\psi(0)|\tilde{X}^{\dagger}e^{i\Lambda^{*}t}X^{\dagger} \tag{3.17}$$

This is the final equation for the density matrix. So, once the eigensystem of the effective Hamiltonian is known, the density matrix can be calculated for all times.

The initial configuration is $|\psi(0)\rangle = |1,0\rangle$, where the electron is in the excited state. The time evolution of the occupation of the initial state is illustrated in figure 3.3. The system undergoes optical Rabi oscillations. The population

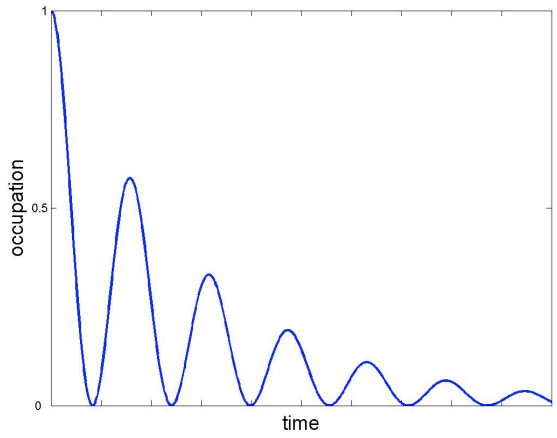

Figure 3.3: Population oscillation of the excited electronic level for time evolution of equation (3.17).

oscillates between the states $|1,0\rangle$ and $|0,1\rangle$ at a frequency $\Omega_R = \sqrt{\Delta^2 + 4g^2}$. This is the Rabi frequency [12]. The oscillation is damped, because the states of the system decay into the ground state by emitting a photon.

3.1.4 The power spectrum $S(\omega)$

We want to evaluate the complete spectrum of the radiation scattered by a qd - cavity system.
The power spectrum is a function of frequency and gives the emitted energy per unit time. It is obtained by the Fourier transform of the two time correlation function of the radiation field. This is known as the Wiener-Khinchin theorem [12],

$$S(\omega) = \frac{1}{2\pi} \lim_{T\to\infty} \frac{1}{T} \int_0^T dt_1 \int_0^T dt_2 \, e^{-i\omega(t_2-t_1)} \left\langle E^-(t_2)E^+(t_1)\right\rangle . \tag{3.18}$$

Because the field operator $E^+(t)$ can be written in terms of the lowering operators $\sigma_-(t)$ and $a(t)$, and $E^-(t)$ in terms of the rising operators $\sigma_+(t)$ and $a^\dagger(t)$, the expectation value can be written as

$$\langle E^-(t_2)E^+(t_1)\rangle \propto \Big(\langle \sigma_+(t_2)\sigma_-(t_1)\rangle + \langle a^\dagger(t_2)a(t_1)\rangle\Big). \tag{3.19}$$

In our consideration, it is possible to evaluate the totally emitted energy, because the system is not driven by an external field. In a driven system, only the energy per unit time is a suitable quantity, because the totally emitted energy is infinite. Therefore, we drop the factor $1/T$, and the totally emitted energy $P(\omega)$ can be calculated by

$$P(\omega) \propto \int_0^\infty dt_1 \int_0^\infty dt_2 \, e^{-i\omega(t_2-t_1)} \Big(\langle \sigma_+(t_2)\sigma_-(t_1)\rangle + \langle a^\dagger(t_2)a(t_1)\rangle \Big). \quad (3.20)$$

The first term gives the emitted energy of the quantum dot, the second one that of the cavity.
The expectation values of equation (3.19), in terms of $t = t_1$, $\tau = t_2 - t_1$, can be transformed using the relation

$$\langle A(t+\tau)B(t)\rangle = \mathrm{tr}\big(\rho(t)A(\tau)B(0)\big) \quad (3.21)$$

This can be evaluated using equation (3.17) and carrying out the trace explicitly. Only one term of the summation survives.
The integrals can be evaluated analytically using

$$\int_0^\infty e^{-izt} dt = \frac{i}{z} \quad \text{if} \quad \mathrm{Im(z)} < 0. \quad (3.22)$$

The constraint $\mathrm{Im(z)} < 0$ makes the integral vanish at the upper boundary. In our system, scattering ensures a negative imaginary part of the complex eigenvalues of the effective Hamiltonian. So, the upper condition is fulfilled.
In components, the spectrum reads

$$P(\omega) = 2Re\left(\sum_i \sum_{\mu\nu} X_{i,\mu} \rho_{\mu\nu} X^\dagger_{\nu,i} \frac{1}{(\lambda_\mu - \lambda^*_\nu)(\lambda^*_\nu - \omega)} \right). \quad (3.23)$$

λ are the entries of the matrix of the eigenvalues Λ. In our calculation the indices i, μ, ν take the values $\{10, 01\}$.

It is possible to separate the emission of the two sources, if we assume the cavity and the quantum dot to emit into different directions. The spectrum of the cavity can be evaluated by dropping the term $\langle \sigma_+(t_2)\sigma_-(t_1)\rangle$ in equation

(3.20). Therefore, the emitted energy is given by

$$P_{\text{cav}}(\omega) = 2Re\left(\sum_{\mu\nu} X_{01,\mu}\rho_{\mu\nu}X^{\dagger}_{\nu,01}\frac{1}{(\lambda_\mu - \lambda^*_\nu)(\lambda^*_\nu - \omega)}\right). \tag{3.24}$$

If the scattering rate κ of the cavity is much larger than the scattering rate γ of the quantum dot, there is nearly no difference between equations (3.23) and (3.24), because the spectrum is dominated by the emission of the cavity.

3.1.5 Strong & weak coupling

When looking at the spectra of the qd - cavity system we notice different regimes, caused by different ratios between the coupling and the damping rates. In the regime of strong coupling, two distinguishable peaks appear in the spectrum. When lowering the coupling strength the peaks come closer and finally only one peak is resolvable.
We will get insight into the mechanism, when looking at the eigenvalues of the effective Hamiltonian of equation (3.10).
When tuning the system to resonance ($\Delta = 0$) the eigenvalues are [1]

$$\lambda_{1,2} = -\frac{i}{4}(\kappa + \gamma) \pm \sqrt{g^2 - \left(\frac{\kappa - \gamma}{4}\right)^2}. \tag{3.25}$$

These are complex values, due to the fact that the effective Hamiltonian is not hermitian. The real part determines the main frequency of the emitted light, the imaginary part the broadening of the peak. For the real part the crucial factor is the coupling g. Therefore, the separation of the eigenenergies is $2g$, which is known as *vacuum Rabi splitting* [17]. Equation (3.4) shows the splitting of the eigenenergies.

To resolve the occurrence of two peaks, the line width $(\kappa + \gamma)/2$ has to be narrower than the splitting $2g$ [8].

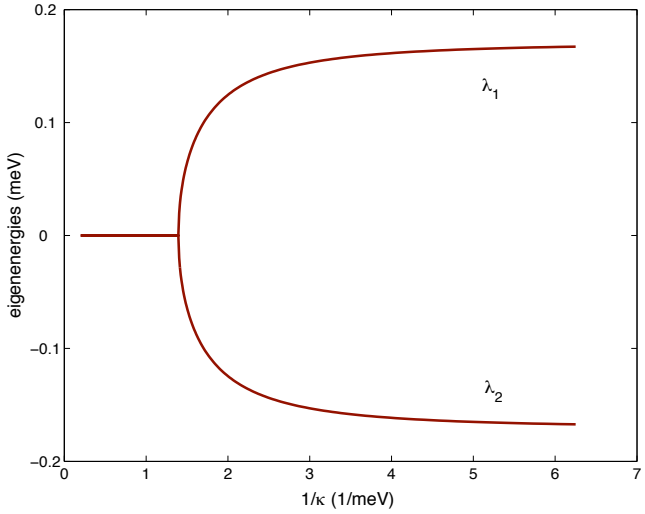

Figure 3.4: Splitting of the eigenenergies in the strong coupling regime for zero detuning. We use the parameters $\gamma = 0.037$ meV, $g = 0.17$ meV

Weak coupling

Weak coupling occurs when the imaginary part exceeds the real part of the eigenvalues,

$$\frac{\kappa + \gamma}{2} > 2g, \tag{3.26}$$

resulting in one visible peak.
Note that there are two different eigenvalues if $(\kappa - \gamma)/4 < g^2$. Otherwise, the eigenvalues are degenerate and the peak maximum is at $\omega = 0$.

Strong coupling

Strong coupling occurs when the real part exceeds the imaginary part of the eigenvalues,

$$\frac{\kappa + \gamma}{2} < 2g. \tag{3.27}$$

The main frequencies of the two peaks are separated far enough to be distinguishable. Two peaks turn up in the spectrum. The appearance of Rabi oscillations, as in figure 3.3, is an effect of strong coupling in the time domain. The power spectrum for the different regimes is illustrated in figure 3.5.

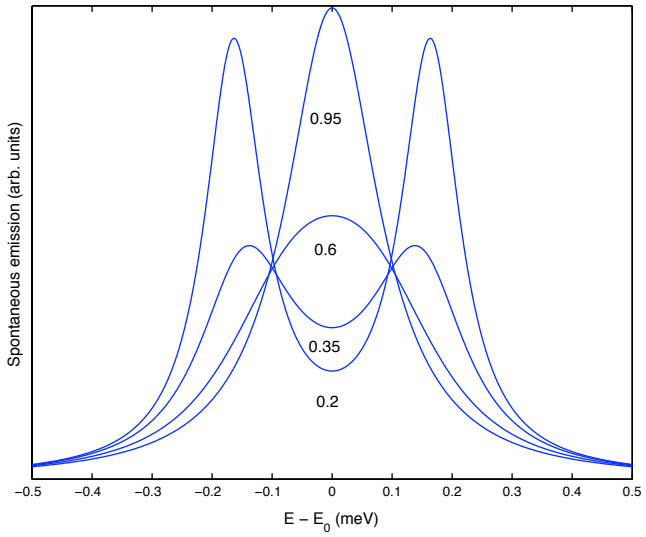

Figure 3.5: The spectrum $P(\omega)$ for different values of κ in meV, zero detuning and the parameters $\gamma = 0.037$ meV, $g = 0.17$ meV. It shows the change from weak to strong coupling.

3.1.6 Dependence on detuning

What happens to the spectrum of a non-resonant ($\Delta \neq 0$) system?
It turns out that the whole spectrum shifts and one peak gets dominant. This is illustrated in figure 3.6.

Constraints to the parameters

Despite an energy mismatch of the photonic and electronic state, population oscillations between these states are possible, but limited by the energy-time uncertainty. In our case, it gives

$$\Delta E \Delta t \approx h. \tag{3.28}$$

The timescale in our problem is defined by the inverse of the coupling g. The uncertainty in energy equals the energy mismatch Δ. Because in our calculations $\hbar = 1$, the upper relation takes the form

$$\Delta \frac{1}{g} \approx 2\pi. \tag{3.29}$$

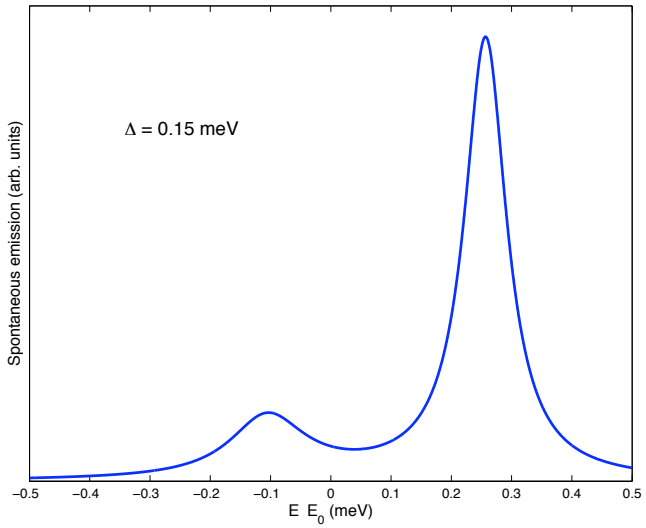

Figure 3.6: Spectrum $P(\omega)$ of the detuned cavity-dot system. The parameters are $\gamma = 0.037$ meV, $g = 0.17$ meV, $\kappa = 0.2$ meV

If the energy mismatch by a given coupling strength is too large, population transfer is strongly suppressed.

Chapter 4

Coherent population transfer among quantum states

The ability to control the transfer of population among specific quantum states is of interest in many applications.
In this section, we discuss the situation in a three level system. The quantum states are coupled via two coherent laser pulses. The coherence characteristics of the light is very important when describing the time evolution. For excitations with coherent light one starts with a time dependent Schrödinger equation, whereas incoherent excitation is described by rate equations [2].
Using a three level system instead of a two level system offers several advantages: it is possible to produce excitation between states of the same parity, for which single-photon transitions are forbidden. Furthermore, the system gets quite insensitive to many of the experimental details of the pulses.
The pump pulse P links the initial state $|1\rangle$ with an intermediate state $|2\rangle$, which in turn couples via a stokes pulse S to a final state $|3\rangle$. The states $|1\rangle$ and $|3\rangle$ are assumed to be stable, whereas the intermediate state $|2\rangle$ is metastable and will undergo spontaneous emission to states in the environment. Figure 4.1 illustrates the relations.
The technique of stimulated Raman adiabatic passage (STIRAP) uses a counterintuitive sequence of the two laser pulses, which turns out to be the natural choice.

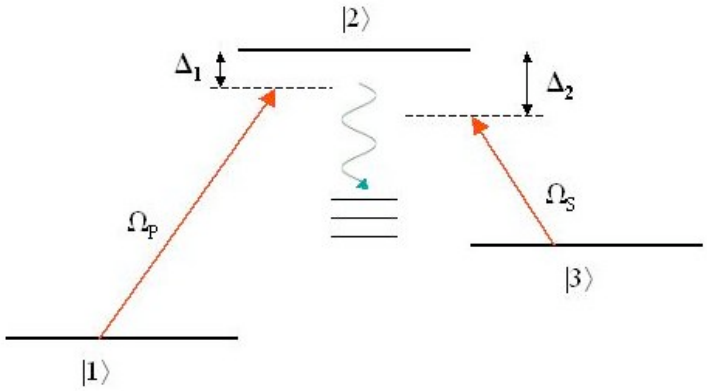

Figure 4.1: Illustration of a three state system

4.1 Stimulated Raman adiabatic passage STIRAP

At first glance it seems intuitive to transfer the population from state $|1\rangle$ to state $|2\rangle$ by first turning on the pump laser, and after some time switch on the stokes laser to bring the population from state $|2\rangle$ to the final state $|3\rangle$. This method is called stimulated emission pumping (SEP). However, this procedure is quite inefficient, since only about a quarter of the population reaches the final state in the end [2].
The efficiency improves significantly if one reverses the ordering of the pulse sequence: The stokes laser acts first, followed by the pump laser. It is important here that the two laser pulses have an appropriate overlap. At first sight this is somewhat unexpected, but a closer look at the eigensystem of the Hamiltonian will give insight [16, 2].

The Hamiltonian of the system in the dipole and rotating wave approximations reads

$$\begin{aligned}\hat{H}(t) &= \sum_{i=1}^{3} E_i|i\rangle\langle i| + \frac{1}{2}\Big[\Omega_P(t)e^{-i\omega_P t}|2\rangle\langle 1| + \Omega_P^*(t)e^{i\omega_P t}|1\rangle\langle 2| \\ &+ \Omega_S(t)e^{-i\omega_S t}|2\rangle\langle 3| + \Omega_S^*(t)e^{i\omega_S t}|3\rangle\langle 2|\Big] \qquad (4.1)\end{aligned}$$

We have assumed that the frequency difference of the pump and stokes laser is large enough, to stimulate the corresponding transition only. The coupling strength between the electronic and photonic system are given by $\Omega_S(t)$ and $\Omega_P(t)$. These are the negative Rabi frequencies. For a complete derivation of the Hamiltonian see appendix B.

In the interaction picture, the Hamiltonian is not explicitly time dependent anymore, and its interaction part reads

$$\hat{H}_I(t) = \frac{1}{2}\begin{pmatrix} 0 & \Omega_P(t) & 0 \\ \Omega_P(t) & 2\Delta_P & \Omega_S(t) \\ 0 & \Omega_S(t) & 2(\Delta_P - \Delta_S) \end{pmatrix}. \tag{4.2}$$

The detuning $\Delta_P = (E_2 - E_1) - \omega_P$ is the energy mismatch of the pump laser and the $|2\rangle - |1\rangle$ transition. $\Delta_S = (E_2 - E_3) - \omega_S$ is the detuning of the stokes laser from the $|2\rangle - |3\rangle$ transition.
The time independent Hamiltonian is achieved by taking the free part of the Hamiltonian as

$$\hat{H}_0 = E_1|1\rangle\langle 1| + (E_1 + \omega_P)|2\rangle\langle 2| + (E_1 + \omega_P - \omega_S)|3\rangle\langle 3|.$$

Spontaneous radiative decay is not included in the Hamiltonian (4.2). We include this terms via the Lindblad formalism and the effective Hamiltonian of equation (3.7).
The time dependent eigenstates of the Hamiltonian of equation (4.2) in the case of two photon resonance $\Delta_P = \Delta_S$ are:

$$\begin{aligned} |a^+\rangle &= \sin\Theta\sin\Phi|1\rangle + \cos\Phi|2\rangle + \cos\Theta\sin\Phi|3\rangle, \\ |a^0\rangle &= \cos\Theta|1\rangle - \sin\Theta|3\rangle, \\ |a^-\rangle &= \sin\Theta\cos\Phi|1\rangle - \sin\Phi|2\rangle + \cos\Theta\cos\Phi|3\rangle, \end{aligned} \tag{4.3}$$

where the time dependent mixing angle is defined by:

$$\tan\Theta = \frac{\Omega_P(t)}{\Omega_S(t)} \tag{4.4}$$

The angle Φ is a known function of the Rabi frequencies and detunings and is not important in our discussion [2].
The eigenstates are called the dressed states. The time dependent eigenvalues of the Hamiltonian are

$$\begin{aligned} \omega^+ &= \Delta_P + \sqrt{\Delta_P^2 + \Omega_P^2 + \Omega_S^2}, \\ \omega^0 &= 0, \\ \omega^- &= \Delta_P - \sqrt{\Delta_P^2 + \Omega_P^2 + \Omega_S^2}. \end{aligned} \tag{4.5}$$

The ability to control the state vector $|\Psi\rangle$ offers the possibility to control the population of the three states. When we look at the eigenstates of equation (4.3), we notice, that the state $|a^0\rangle$ is always free of any contribution of the leaky state $|2\rangle$. That means, this state can not emit a photon and is therefore called the dark state. It is the appropriate vehicle to transfer the population.
In the beginning, our system is in the state $|\Psi\rangle = |1\rangle$, which is, at this time, identical to the dark state $|a^0\rangle$. When turning on the stokes laser, it can not transfer population, since it couples the yet empty states $|2\rangle$ and $|3\rangle$. But this does not mean it has no effect: In the case of resonant one photon transition ($\Delta_P = \Delta_S = 0$), the eigenstates of equation (4.5) are degenerate in the beginning. Turning on the stokes laser cancels the degeneracy of the eigenstates. This splitting of the energies plays an important role in the further process.
After some time delay, the pump laser is activated and changes the mixing angle of equation (4.4) from 0° to 90°. This means the state $|a^0\rangle$ is rotated from state $|1\rangle$ to state $|3\rangle$. To achieve complete population transfer to the final state $|3\rangle$, the state vector $|\Psi\rangle$ has to follow the motion of $|a^0\rangle$ adiabatically. To satisfy this condition, the coupling has to be adequate.
Inefficient coupling may occur, when the Rabi frequencies are to small. In that case, the field induced splitting of the energies $|\omega^\pm - \omega^0|$ is small compared to the matrix elements for non adiabatic coupling $\langle a^\pm | \dot{a}^0 \rangle$. That means, transitions from state $|a^0\rangle$ to the states $|a^\pm\rangle$ are possible during the process. The adiabatic condition can be simplified to [2]

$$\Omega_{eff} \Delta\tau > 10 \tag{4.6}$$

where $\Omega_{eff} = \sqrt{\Omega_P^2 + \Omega_S^2}$ is the rms (root mean square) Rabi frequency and $\Delta\tau$ the overlap-time of the stokes and pump laser pulses. The value 10 is estimated from numerical simulation studies and from experiments [2].
To avoid non-adiabatic coupling, the time delay between the pulses is also a relevant factor. It has been shown that the mixing angle should reach $\pi/4$ when Ω_{eff} reaches its maximum value. For Gaussian-beam pulse shape, the delay should be equal to the laser pulse width [5]. Figure 4.3 shows the transfer efficiency to the final state as a function of the delay time. If the delay time exceeds the point B, Ω_{eff} has two maxima, and the efficiency decreases. This situation is discussed in appendix C. The optimal delay time T_{opt} is given by

$$\sigma \geq t_{\text{opt}} \geq \sqrt{2} \cdot \sigma \tag{4.7}$$

The transfer efficiency is not very sensitive to the single photon detuning, but it is important, that the two photon resonance condition $\Delta_P = \Delta_S$ holds.

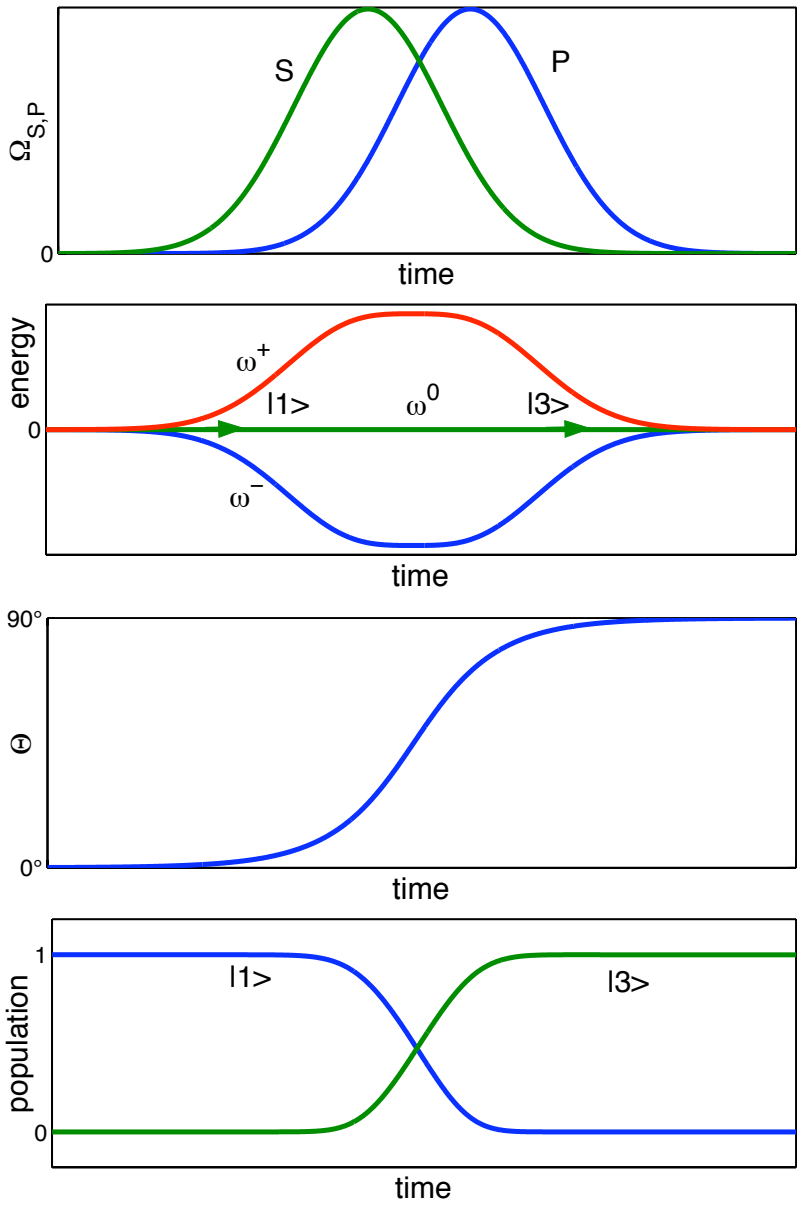

Figure 4.2: Time dependence of the laser pulses, eigenvalues, mixing angle and the population of the initial and final states for optimal pulse delay.

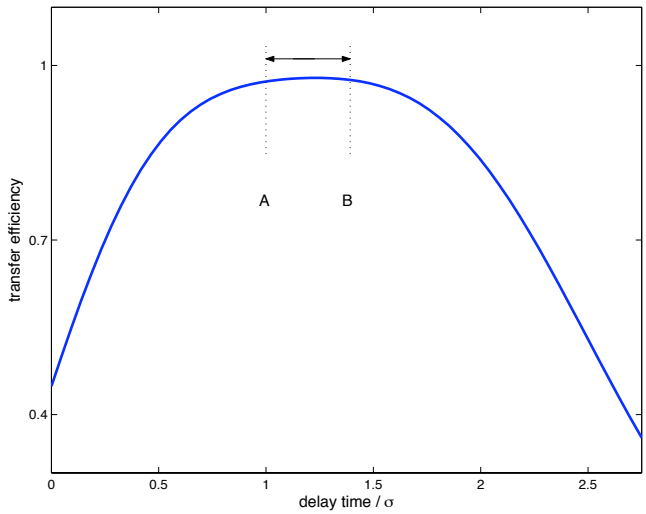

Figure 4.3: Transfer efficiency as a function of the delay time. The optimal delay time lies between $A = \sigma$ and $B = \sqrt{2} \cdot \sigma$.

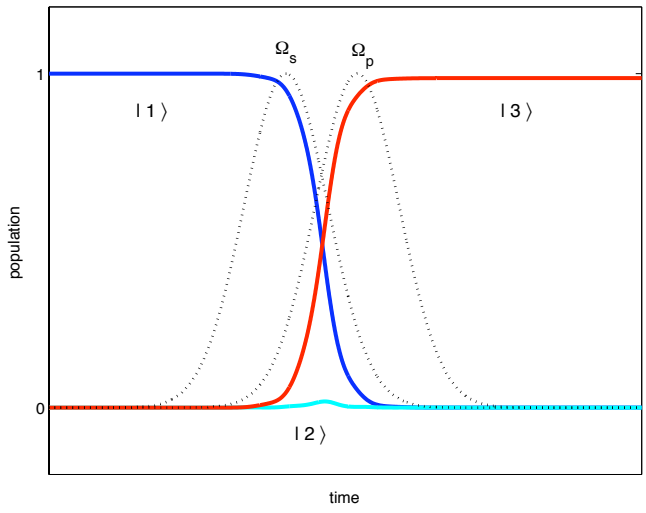

Figure 4.4: The simulation of the STIRAP process shows, that the metastable intermediate state $|2\rangle$ is rarely occupied.

Chapter 5

Population transfer in a driven quantum dot - cavity system

Now, we want to combine the results of the chapters 3 and 4.
The system we are looking at, consists of a three-level quantum dot interacting with a cavity mode. The quantum dot is driven by an external laser field. This looks quite similar to the STIRAP system of chapter 4. The only difference is, that the stokes laser is replaced by a cavity.
The aim stays the same: We want to bring the population from the electronic ground state to the final state of the three level system. Figure 5.1 illustrates the situation.

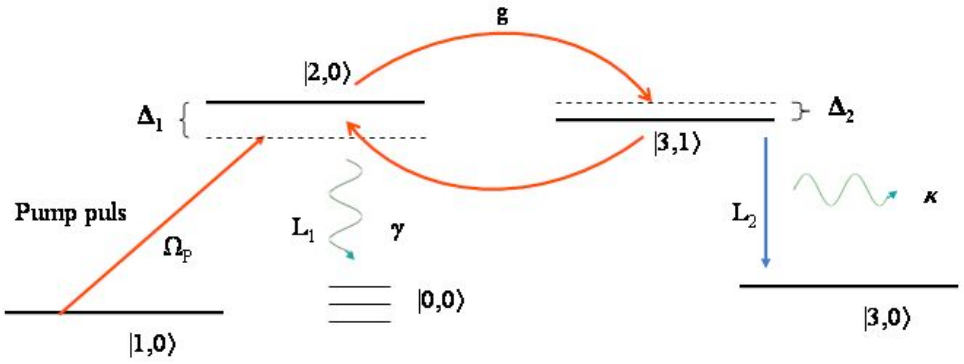

Figure 5.1: Illustration of a driven qd - cavity system

5.1 The Hamiltonian of the system

We consider an electronic 3-state system, coupled to a single cavity field mode, driven by an external field. The Hamiltonian of the system in the rotating wave approximation reads

$$\begin{aligned}\hat{H}(t) &= \sum_{i=1}^{3} E_i|i\rangle\langle i| + \omega_C a^\dagger a \\ &+ \frac{1}{2}\left(\Omega_P(t)e^{-i\omega_P t}|2\rangle\langle 1| + \Omega_P^*(t)e^{i\omega_P t}|1\rangle\langle 2|\right) \\ &+ g\left(|2\rangle\langle 3|a + |3\rangle\langle 2|a^\dagger\right), \end{aligned} \tag{5.1}$$

The terms in the first line of equation(5.1) give the energy of the electronic and photonic levels, where $a^\dagger$ and a are the creation and annihilation operators of the cavity photons. The terms in the second line describe the interaction of the classical driving field with the electronic system, where ω_P is the frequency of the field and Ω_P is the Rabi frequency. The terms in the last line take the coupling of the electronic states and the cavity photons into account, where g is the coupling constant.
The Hilbert space we are working in can be written as a direct product of the electronic and the photonic parts as in equation (3.2). The basis set is a combination of the basis sets of the subsystems explained in equation (3.3) and reads

$$\{|1,0\rangle, |2,0\rangle, |3,1\rangle, |3,0\rangle, |0,0\rangle\}.$$

The first entry of each vector corresponds to the electronic state, the second one gives the number of photons in the cavity. In our calculation, there is only a single cavity photon allowed. The states $|3,0\rangle$ and $|0,0\rangle$ can only be reached via scattering processes, described by the Lindblad operators. Therefore, the Hamiltonian of equation (5.1) can be written in the 3-dimensional basis

$$\{|1,0\rangle, |2,0\rangle, |3,1\rangle\}.$$

To get rid of the time dependence of the Hamiltonian, we change into the interaction picture. The interaction part of the Hamiltonian in the interaction

picture takes the form

$$\hat{H}_{1I} = \frac{1}{2}\begin{pmatrix} 0 & \Omega_P & 0 \\ \Omega_P^* & 2\Delta_1 & 2g \\ 0 & 2g & 2(\Delta_1 - \Delta_2) \end{pmatrix}, \tag{5.2}$$

where $\Delta_1 = (E_2 - E_1) - \omega_P$ is the energy mismatch of the $1 \to 2$ transition and the driving field. $\Delta_2 = (E_2 - E_3) - \omega_C$ is the energy mismatch of the cavity and the $2 \to 3$ transition.
To arrive at equation (5.2) the free part of the Hamiltonian has to be chosen as

$$\hat{H}_0 = E_1|1,0\rangle\langle 1,0| + (E_1 + \omega_P)(|2,0\rangle\langle 2,0| + |3,1\rangle\langle 3,1|). \tag{5.3}$$

5.1.1 Including scattering

The scattering processes are taken into account by introducing Lindblad terms. We consider two scattering channels

$$\hat{L}_1 = \sqrt{\gamma}|0,0\rangle\langle 2,0| \tag{5.4}$$

$$\hat{L}_2 = \sqrt{\kappa}|3,0\rangle\langle 3,1| \quad . \tag{5.5}$$

The first one describes the spontaneous decay of the excited electronic level $|2\rangle$ into states of the environment. The second one denotes that the excited photonic state can also decay, because the cavity is leaking.
We write the dynamics of the density matrix, described by the Lindblad master equation (2.28) as

$$\frac{d\hat{\rho}}{dt} = \frac{1}{i\hbar}\left[\hat{H_{\text{eff}}}, \hat{\rho}\right] - \sum_k \hat{L}_k \hat{\rho}(0) \hat{L}_k^\dagger. \tag{5.6}$$

The coherent dynamics and the outscattering terms are included in the effective Hamiltonian $\hat{H}_{\text{eff}}$ defined in equation (3.7). The second term on the right side describes the inscattering contributions. In contrast to chapter 3, we do not drop these terms here, since we are interested in the occupation of the final state $|3,0\rangle$.

5.2 Population transfer

Within this system, we want to transfer the population from the electronic ground state $|1\rangle$ to the final state $|3\rangle$. A very efficient method to transfer population in a three state system is the STIRAP process, which is explained in chapter 4. It uses two coherent laser pulses, arranged in counterintuitive order. The only difference in the current system is, that the transition from state $|2\rangle$ to state $|3\rangle$ is stimulated by the cavity and not by the stokes laser. The switch off process of the stokes pulse plays a central role in the STIRAP process. Here, we have no ability to control the light field, because there is no way to switch off the interaction with the cavity.
In spite of this, is there a way to transfer the population to the final state efficiently? It turns out, that the scattering process, described by the Lindblad operator L_2, permits to transfer the population.

What's happening? In the beginning, the cavity couples the intermediate state with the final state. This equals the turn-on procedure of the stokes laser in the STIRAP process. Then, the pump pulse is activated and the population can be transferred. After some time, the pump pulse is switched off, but the interaction with the cavity still remains. When we look at the mixing angle of equation (4.4) we find

$$\tan\Theta = \frac{\Omega_P(t)}{2g}. \tag{5.7}$$

Here, the Rabi frequency of the stokes laser is substituted by two times the coupling constant. To transfer the population completely, the mixing angle has to take the value $\pi/2$ in the end. Here, Θ reaches $\pi/4$ before it returns to 0 again. Figure 5.2 shows the motion of the mixing angle. This means, the motion system state vector $|\psi\rangle$ is

$$|1\rangle \quad \rightarrow \quad \frac{1}{\sqrt{2}}\big(|1\rangle + |3\rangle\big) \quad \rightarrow \quad |1\rangle.$$

So, if there was no outscattering from the level $|3,1\rangle$, all the population would be transfered back to the ground state. This situation is illustrated in figure 5.3.

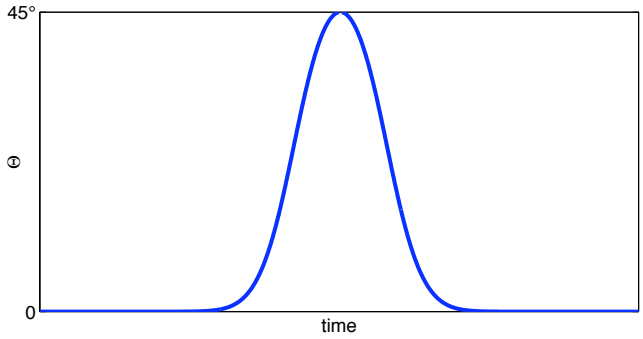

Figure 5.2: The mixing angle in the modified STIRAP process.

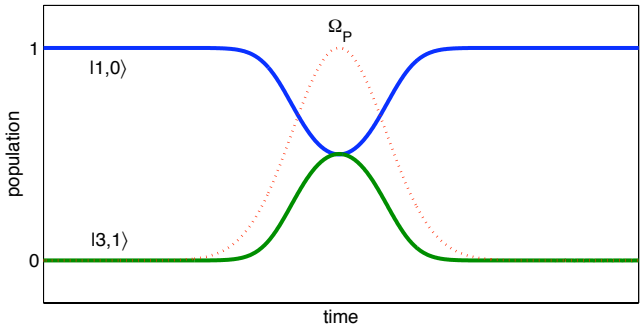

Figure 5.3: Population of the states for $\kappa = 0$.

In our consideration, we did not include spontaneous emission of the cavity photon. If we do, the situation changes dramatically. The decay of the cavity photon empties the level $|3,1\rangle$ during the transfer process and brings the population to the final state $|3,0\rangle$. The coupling of the cavity and the electronic states is still there, but at the moment the state vector returns to the ground state, the states of the system are not populated anymore. This can be seen in figure 5.4.
If the damping rate of the cavity is large enough, all the population ends up in $|3,0\rangle$. Re-excitation from this state is not possible.

5.2.1 Dependence on detuning

So far, we only considered the resonant case ($\Delta_1 = \Delta_2 = 0$). Now we want to check how the efficiency of the process is determined by the detuning. It turns out that the population transfer in the STIRAP process does not depend very

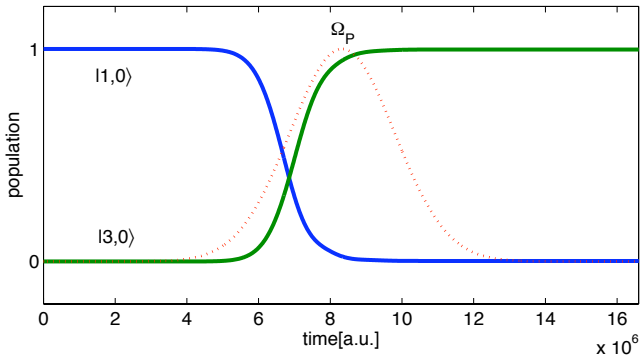

Figure 5.4: Population transfer in a driven qd-cavity system, plotted in atomic units. The resonance condition ($\Delta_1 = \Delta_2 = 0$) is fulfilled. The other parameters are taken from [6]: $\gamma = 0.05$ μeV, $\kappa = 100$ μeV, $g = 100$ μeV, $\sigma = 35$ ps.

much on detuning, as long as the two-photon resonance condition ($\Delta_1 = \Delta_2$) is fulfilled.

What's the situation here? Figure 5.5 shows the population of the final state as a function of detuning. As before, the process works very well as long as the detunings Δ_1 and Δ_2 are the same. This situation is given by the straight line from the left top to the right bottom.

When moving away from the two-photon resonant case, the efficiency decreases. We notice, that the system is more sensitive to the detuning of the laser Δ_1, than to the detuning of the cavity Δ_2.

5.3 Restarting the process

In our system, population transfer from the initial to the final state works quite well. Now, we want to start the process again. Therefore, the population has to be transferred to the ground state again. We achieve this objective, taking phonon scattering into account. The interaction with phonons is described via an additional scattering channel and an other Lindblad operator

$$L_3 = \sqrt{\gamma_{\text{ph}}}|1\rangle\langle 3|. \tag{5.8}$$

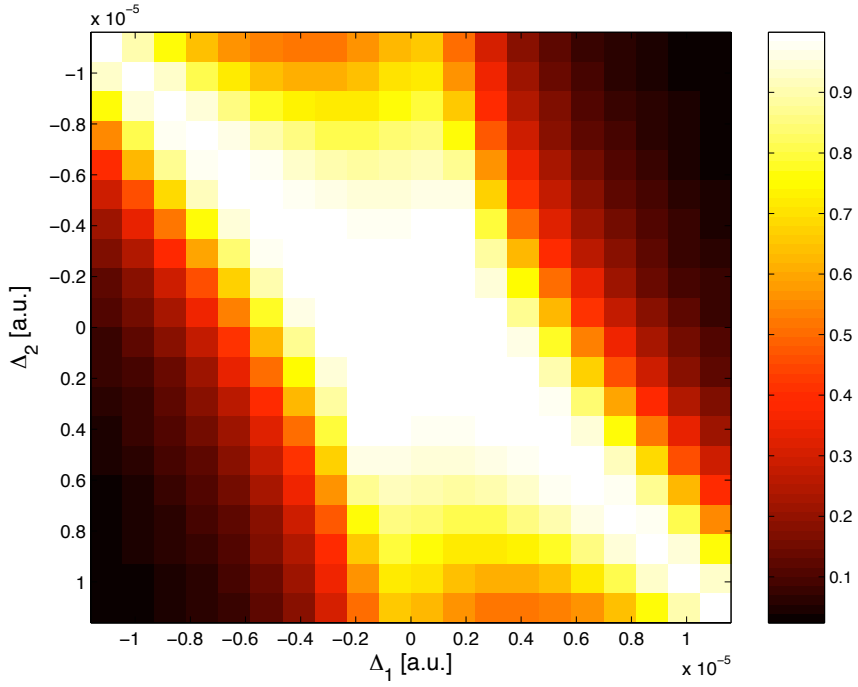

Figure 5.5: Population of the final state as a function of detuning. Plotted in atomic units. The other parameters are taken as in figure 5.1.

Including this scattering channel, the basis we are working in has to be extended to

$$\{|1,0\rangle, |1,1\rangle, |2,0\rangle, |2,1\rangle, |3,0\rangle, |3,1\rangle, |0,0\rangle, |0,1\rangle\},$$

according to the fact, that the Lindblad operator L_3 can populate the state $|1,1\rangle$ when acting on $|3,1\rangle$. If the phonon scattering rate γ_{ph} is much smaller than the photon scattering rate κ, the states $|2,1\rangle$ and $|0,1\rangle$ are not populated. In this case we drop them in our calculations. It is important, that the condition $\gamma_{\text{ph}} \ll \kappa$ is fulfilled. Otherwise the transfer mechanism is disturbed too much and the population can not be transferred efficiently.

A simulation of one cycle with small phonon scattering rate is shown in figure 5.6. As can be seen, nearly all of the population ends up in the ground state. A small fraction is lost, when the adiabatic-following-condition of the state vector is not exactly fulfilled. Therefore, the metastable state $|2\rangle$ is populated during the transfer process, which couples to the environment.

After the population has been transferred back to the ground state, the process

can be started again. Applications using a few cycles are presented in chapter 6.

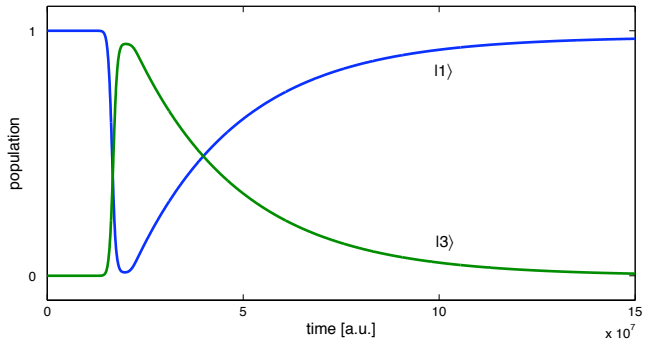

Figure 5.6: Population of the initial and final state including phonon scattering to the ground state. The parameters are: $\Delta_1 = 20$ μeV, $\Delta_2 = 20$ μeV, $\gamma = 6$ μeV, $\kappa = 100$ μeV, $\gamma_{\mathrm{ph}} = 1$ μeV, $g_0 = 100$ μeV, $\sigma = 45$ ps

Chapter 6

QD-based photon entanglement

There are many different applications using qd-cavity systems. Apart from the evident one - transferring population to a specific state - the scattered cavity photon is of major interest: the quantum dot - cavity system can be used as a *single photon source*. These single photons can be used to produce entangled states or nano lasers [14].
The generated electromagnetic wave has a well-defined shape. Also the output direction can be fixed by experimental arrangement, which makes optical access to it easy.
In the following chapter, we explain how an entangled state can be produced, using a cavity QED system.

6.1 Producing entangled states

In this section we want to give an idea of how this system can be used in order to produce maximally entangled states. For this reason, we consider two of the cavity-dot systems described in chapter 5. We assume the electronic states of the two cycles to have different energies. This can be realized using e.g. the spin of the electron. The photonic crystal slab cavity we have in mind shows a vertically and a horizontally polarized mode. This is illustrated in figure 6.1.
The idea is to couple each of the two modes only with one electronic transition. That means, that the spin-up cycle always emits a vertically polarized photon (V), while the spin-down cycle always produces a horizontally polarized photon.

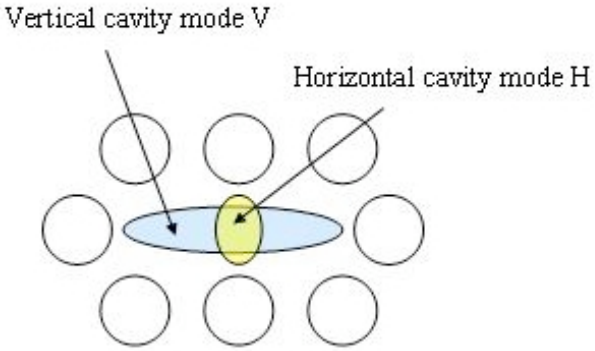

Figure 6.1: A photonic crystal slab cavity normally shows a vertically (V) and a horizontally (H) polarized mode with different energies.

Now, what happens to the state vector $|\psi\rangle$, if we start with a mixed ground state $\frac{1}{\sqrt{2}}\big(|\uparrow\rangle + |\downarrow\rangle\big)$? After one round we get

$$\frac{1}{\sqrt{2}}\big(|\uparrow\rangle + |\downarrow\rangle\big) \quad \stackrel{1}{\rightarrow} \quad \frac{1}{\sqrt{2}}\big(|\uparrow H\rangle + |\downarrow V\rangle\big). \tag{6.1}$$

Phonon scattering (section 5.3) brings the state vector of the system back to the initial state. When $|\psi\rangle$ has reached the ground state again, the process can be started again and again...
We get:

$$\begin{aligned} \frac{1}{\sqrt{2}}\big(|\uparrow\rangle + |\downarrow\rangle\big) \quad &\stackrel{1}{\rightarrow} \quad \frac{1}{\sqrt{2}}\big(|\uparrow H\rangle + |\downarrow V\rangle\big) \\ &\stackrel{2}{\rightarrow} \quad \frac{1}{\sqrt{2}}\big(|\uparrow HH\rangle + |\downarrow VV\rangle\big) \\ &\stackrel{3}{\rightarrow} \quad \frac{1}{\sqrt{2}}\big(|\uparrow HHH\rangle + |\downarrow VVV\rangle\big) \\ &\vdots \end{aligned} \tag{6.2}$$

If we somehow get rid of the extra information about the spin, we end up with a maximally entangled state.

To make this procedure work, it is essential that the spin up electron only interacts with the vertically polarized cavity mode, and the spin down electron couples only to the horizontally polarized cavity mode.

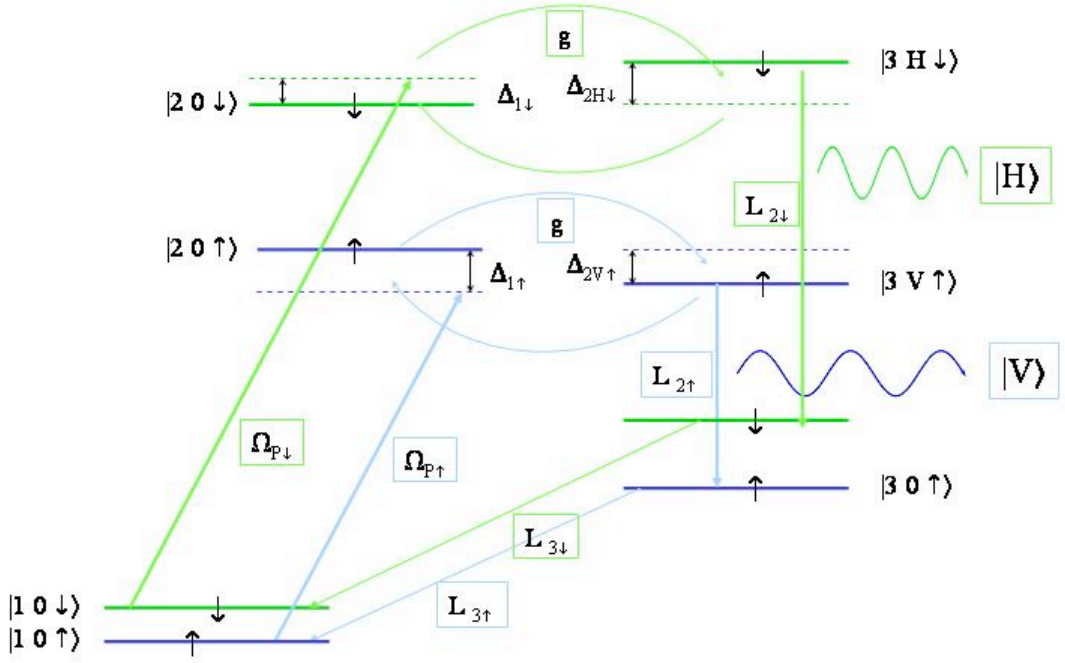

Figure 6.2: The energy levels of the two cycles.

This can be achieved, using the low transfer efficiency for large detuning (see figure 5.5). To simplify the following discussion we introduce the notation:

$$\begin{aligned} \Delta_{1\uparrow} &= (E_{2\uparrow} - E_{1\uparrow}) - \omega_{P\uparrow} & \Delta_{1\downarrow} &= (E_{2\downarrow} - E_{1\downarrow}) - \omega_{P\downarrow} \\ \Delta_{2\,V\uparrow} &= (E_{2\uparrow} - E_{30\uparrow}) - \omega_V & \Delta_{2\,H\downarrow} &= (E_{2\downarrow} - E_{30\downarrow}) - \omega_H \\ \Delta_{2\,H\uparrow} &= (E_{2\uparrow} - E_{30\uparrow}) - \omega_H & \Delta_{2\,V\downarrow} &= (E_{2\downarrow} - E_{30\downarrow}) - \omega_V \end{aligned} \quad (6.3)$$

These are the various detunings of the system. An explanation can be found in figure 6.3.
The transfer of population works well, if the two photon resonance condition $\Delta_1 = \Delta_2$ is fulfilled and it is strongly damped if we deviate from resonance. This has been shown in section 5.2.1. Therefore, optimal conditions to produce maximally entangled states are given by:

$$\begin{aligned} \Delta_{1\uparrow} &= \Delta_{2\,V\uparrow}, & \Delta_{1\downarrow} &= \Delta_{2\,H\downarrow}, \\ \Delta_{1\uparrow} &\neq \Delta_{2\,H\uparrow}, & \Delta_{1\downarrow} &\neq \Delta_{2\,V\downarrow}. \end{aligned}$$

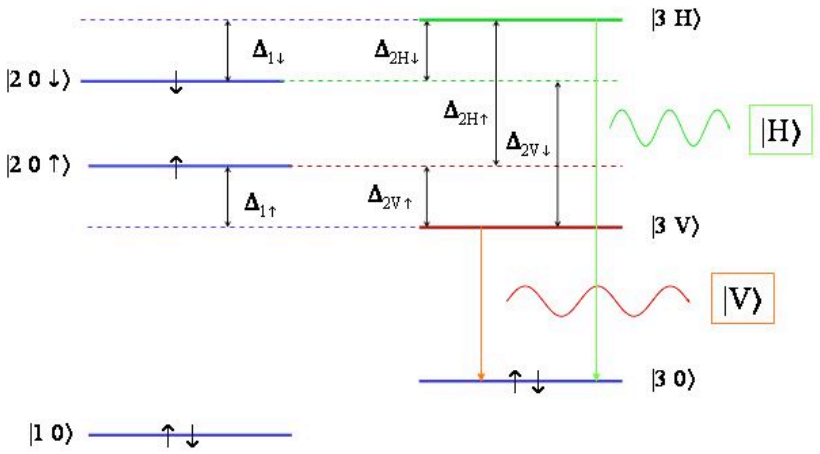

Figure 6.3: A simple model of the energy levels. The spin-up and spin-down alignments of the ground and final state are degenerate.

This can be achieved, if the energy splitting of the states $|2\,0\,\uparrow\rangle$ and $|2\,0\,\downarrow\rangle$ is large enough. The splitting of the other electronic levels is not needed for this purpose. To maximize the detuning of the unwanted transitions it is useful to choose the energy mismatch of the lasers $\Delta_{1\uparrow} > 0$ and $\Delta_{1\downarrow} < 0$. Then the detuning of the unwanted transitions reaches a maximum. Figure 6.3 shows a simple model of the energy levels and the detunings for degenerate ground and final state.

In our simulations we tuned the wanted transitions to the two photon resonance and took the other values $\Delta_{1\uparrow} = 0.15$ meV and $\Delta_{2\,H\uparrow} = -0.30$ meV. These conditions fix the splitting of the metastable state $|2\rangle$ to 0.15 meV.
For these parameters and equal scattering rate for H and V modes, the population of the wanted state $|3\,V\,\uparrow\rangle$ is 78 times larger than the population of the state $|3\,H\,\uparrow\rangle$. That means, that statistically, every 78-th round the spin-up electron produces a H-photon. A larger splitting of the state $|2\rangle$ increases this value. For a splitting of 45 meV the factor turns out to be 181.
The same parameters with different sign are taken for the spin-down cycle.

Notes

- In our considerations we did not include the possibility of a spin flip.
- Performing a projective measurement we can get rid of the extra information about the spin. Measuring the spin into an orthogonal direction lifts the entanglement concerning the material part.

Conclusion

In this thesis, we have investigated the dynamics of a quantum dot - microcavity system in the strong coupling regime. The description via the density matrix turned out to be very useful, since the Lindblad master equation offers a practicable way to evaluate the time evolution.
With the STIRAP method, we found an efficient way to transfer population between the excitonic states of the quantum dot. Within the cavity QED-system, we were able to transfer population with a modified STIRAP process. The cavity can substitute the stokes laser, if the outscattering is strong enough. In applications, this scattered photon is of major interest: the system can be used as a *single photon source*. We turned special attention to the dependency of the transfer efficiency on the detuning of the system, and found a strong sensibility to variances from the two photon resonance condition. This could be used to figure the production of entangled states with a cavity QED-system.

Appendix A

Conditions for a quantum operation

A.1 Positivity

A mapping $\mathcal{E}$: $\hat{\rho} \to \hat{\rho}'$ is positive, if it conserves the non-negativity of the operator $\hat{\rho}$. That means, if $\hat{\rho}$ is positive, so is $\hat{\rho}' = \mathcal{E}(\hat{\rho})$.

An operator $\hat{\rho}$ is defined to be positive, if for an arbitrary vector $|\psi\rangle$ in state space

$$\langle\psi|\hat{\rho}|\psi\rangle \geq 0. \tag{A.1}$$

A positive operator is hermitian. Furthermore, it has real and positive eigenvalues.
Positivity is an attribute of the density operator.

A.2 Complete positivity

Now we extend our Hilbert space $\mathcal{H}_A$ to the tensor product $\mathcal{H}_A \otimes \mathcal{H}_B$. A mapping $\mathcal{E}_A$ is complete positive on $\mathcal{H}_A$, if $\mathcal{E}_A \otimes \mathcal{I}_B$ is positive for all such extensions. $\mathcal{I}_B$ denotes the identity map on the subsystem B.
Complete positivity is an important property of a quantum operation. It results from the requirement that, if the subsystem A evolves and B does not, any

density matrix of the combined system evolves to another valid density matrix. The transposition operator is an example for a positive operator which is not complete positive. For further reading see [9, 10].

Appendix B

The rotating wave approximation

The rotating wave approximation is often used in the description of atom-field interactions. Within a classical description of the field, we drop the fast rotating terms in the Hamiltonian. When quantizing the radiation field, the rotating wave approximation corresponds to dropping the energy non conserving terms in the Hamiltonian.

B.1 Semiclassical theory

We consider a two level atom driven by a classical radiation field of frequency ω_L. The interaction energy of an electrical dipole with the external light field in the dipole approximation is given by

$$\hat{H}_1 = -\vec{D} \cdot \vec{E}. \tag{B.1}$$

$\vec{D}$ is the electric dipole operator, which can be written as

$$\vec{D} = \vec{d}\sigma_- + \vec{d}^*\sigma_+. \tag{B.2}$$

$\sigma_+ = |e\rangle\langle g|$ and $\sigma_- = |g\rangle\langle e|$ are the raising and lowering operators. $\vec{d} = \langle g|\vec{D}|e\rangle$ is the transition matrix element of the dipole operator. $|e\rangle$ denotes the excited state, $|g\rangle$ the ground state of the electronic system. The electric field strength

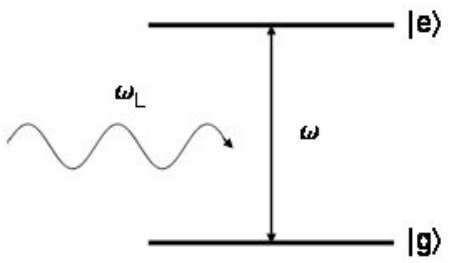

Figure B.1: Interaction of a two level atom with a single mode field.

of the driving field can be written as

$$\vec{E}(t) = \vec{\varepsilon} e^{-i\omega_L t} + \vec{\varepsilon}^* e^{i\omega_L t}, \tag{B.3}$$

where $\vec{\varepsilon}$ is the amplitude of the electric field. The total Hamiltonian of the system is given by

$$\hat{H} = \hat{H}_0 + \hat{H}_1 = \hbar\omega_e |e\rangle\langle e| - \vec{D} \cdot \vec{E}, \tag{B.4}$$

where $\hbar\omega_e$ is the energy of the excited electronic level. The energy of the electronic ground state is taken to zero. In the interaction picture, the interaction part of the Hamiltonian reads

$$\begin{aligned}
\hat{H}_{1I}(t) &= \hat{U}_0^\dagger(t,t_0)\hat{H}_I\hat{U}_0(t,t_0) && \text{(B.5)}\\
&= -e^{i/\hbar\hat{H}_0 t}(\vec{d}\sigma_- + \vec{d}^*\sigma_+)(\vec{\varepsilon}e^{-i\omega_L t} + \vec{\varepsilon}^* e^{i\omega_L t})e^{-i/\hbar\hat{H}_0 t} && \text{(B.6)}\\
&= -\vec{d}\sigma_-(\vec{\varepsilon}e^{-i\omega_L t} + \vec{\varepsilon}^* e^{i\omega_L t})e^{-i\omega t} - \vec{d}^*\sigma_+(\vec{\varepsilon}e^{-i\omega_L t} + \vec{\varepsilon}^* e^{i\omega_L t})e^{i\omega t} && \text{(B.7)}
\end{aligned}$$

The terms in the Hamiltonian are evolving at two different time scales. The slowly rotating terms evolve at the frequency $\omega - \omega_L$. The terms, which evolve at the frequency $\omega + \omega_L$ are the fast rotating terms. Dropping the rapidly rotating terms in the Hamiltonian is called the rotating wave approximation. The interaction part of the rotating wave Hamiltonian in the interaction picture reads

$$\hat{H}_{1I}^{RWA}(t) = -\frac{1}{2}\left(\sigma_+\Omega e^{i\Delta t} + \sigma_-\Omega^* e^{-i\Delta t}\right), \tag{B.8}$$

where $\Omega = 2\vec{\varepsilon}\cdot\vec{d}^*$ is the Rabi frequency and $\Delta = \omega - \omega_L$ is the difference of the frequencies. Carrying out the back-transformation with the unitary operator $\hat{U}(t,t_0)$, we arrive at the Schrödinger picture interaction Hamiltonian in the rotating wave approximation

$$\begin{aligned}\hat{H}_1^{RWA}(t) &= \hat{U}(t,t_0)\hat{H}_{1I}^{RWA}(t)\hat{U}^\dagger(t,t_0)\\ &= -\frac{1}{2}\left(\sigma_+\Omega e^{-i\omega_L t} + \sigma_-\Omega^* e^{i\omega_L t}\right),\end{aligned} \tag{B.9}$$

B.2 Quantum theory

We consider an atom interacting with a cavity confined electric field. The electric field operator at the position of the atom in the dipole approximation reads [12]

$$\vec{E} = \sum_{\vec{k}} \hat{\epsilon}_{\vec{k}}\varepsilon_{\vec{k}}(a_{\vec{k}} + a_{\vec{k}}^\dagger), \tag{B.10}$$

where $\varepsilon_{\vec{k}} = (\hbar\omega_{\vec{k}}/2\epsilon_0 V)^{1/2}$ and V is the volume of the resonator. The polarization vectors are chosen to be real. $a^\dagger$ and a are the photonic creation and annihilation operators.
The interaction energy $-\vec{D}\cdot\vec{E}$ can be described in the dipole approximation by

$$\hat{H}_1 = \hbar\sum_{\vec{k}} g_{\vec{k}}(a_{\vec{k}} + a_{\vec{k}}^\dagger)(\sigma_- + \sigma_+), \tag{B.11}$$

where

$$g_{\vec{k}} = -\frac{\vec{d}\cdot\hat{\epsilon}_{\vec{k}}\varepsilon_{\vec{k}}}{\hbar} \tag{B.12}$$

is the coupling between the dipole and the cavity modes. The dipole transition matrix elements are assumed to be real ($\vec{d} = \vec{d}^*$).
The interaction part of the Hamiltonian consists of four terms. The terms $\sigma_+ a$ and $\sigma_- a^\dagger$ are processes where the energy is conserved. The first brings the electron from the ground state to the excited state and annihilates a photon. The second process takes the electron to the ground state and creates a photon. The other two processes $\sigma_- a$ and $\sigma_+ a^\dagger$ are the energy non conserving terms.

The first one results in the loss of energy of approximately $2\hbar\omega$, the second one in the gain of $2\hbar\omega$. Neglecting the energy non conserving terms corresponds to the rotating wave approximation.

Appendix C

Optimal pulse delay time for Gauss pulses

As shown in Ref. [5] and discussed in Ref. [2], for Gaussian beam pulse shape the optimal delay time of the pulses is in the order of the pulse width. We have shown in figure 4.3 that the optimal delay time lies between σ and $\sqrt{2} \cdot \sigma$. The delay time has to be long enough to ensure the motion of the mixing angle and evolution of the state vector from $|1\rangle$ to $|3\rangle$. On the other hand, if the the delay time is too large, Ω_{eff} has fallen below its maximum value, when the changing of the mixing angle has its maximum. This supports transitions to the metastable state $|2\rangle$, since the splitting of the eigenstates is determined by Ω_{eff}. In this case, Ω_{eff} has two peaks. This is shown in the last plot of figure C.2.

A Gaussian shape is described by the function

$$f(t) = Ae^{-\frac{1}{2}(\frac{t-t_0}{\sigma})^2}, \tag{C.1}$$

where σ is the standard deviation and t_0 fixes the center of the peak.

The upper limit of the delay time Δt_{max} can be found by evaluating the second derivative of Ω_{eff}. It turns out to be

$$\Delta t_{\text{max}} = \sqrt{2} \cdot \sigma, \tag{C.2}$$

which is equal to the time the Gauss pulse takes to reduce to A/e. This is illustrated in figure C.1.

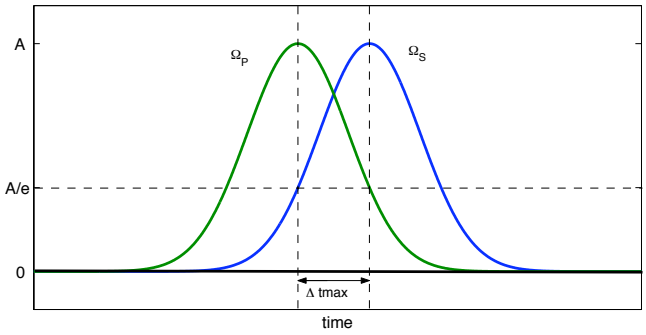

Figure C.1: The maximum delay time for efficient transfer is determined by $\Delta t_{\max} = \sqrt{2} \cdot \sigma$.

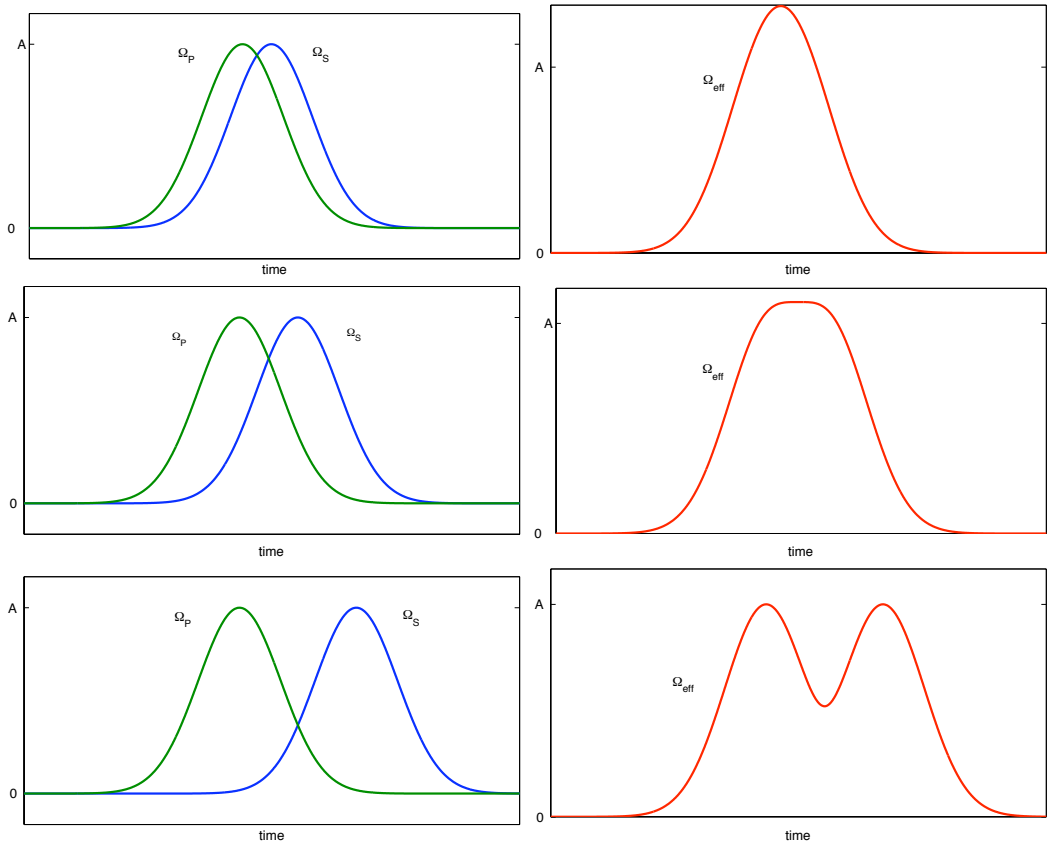

Figure C.2: Illustration of the envelope function $\Omega_{\text{eff}} = \sqrt{\Omega_{\text{S}}^2 + \Omega_{\text{P}}^2}$ for different delay times. The first one has a short delay time: $\Delta t = \Delta t_{\max}/2$. The second one illustrates the limit: $\Delta t = \Delta t_{\max}$. The third one has a large delay time: $\Delta t = 2 \cdot \Delta t_{\max}$.

Appendix D

Atomic units

In 1959 H. Shull and G. G. Hall suggested the use of atomic units (a.u.) for quantum-mechanical calculations [13]. The three basic quantities of the system are the electron charge e, the electron mass m and the reduced Planck constant $\hbar$. The other units (energy, length, etc.) can be derived from them. Atomic units are convenient for atomic physics, electromagnetism and QED. The following six physical constants are unity in this system of units:

Electron charge	$e = 1$	Bohr radius	$a_0 = 1$
Electron mass	$m_e = 1$	Hartree energy	$H = 1$
Reduced Planck constant	$\hbar = 1$	Coulomb constant	$k_c = 1$

The unity of the Coulomb constant $k_c = 1/(4\pi\epsilon_0)$, results from the use of Gaussian units, where $\epsilon_0 = 1/(4\pi)$.

Unit name	**Symbol**	**SI value**
Electron mass	m_e	$9.109 \cdot 10^{-31} kg$
Bohr radius	a_0	$5.292 \cdot 10^{-11} m$
Elementary charge	e	$1.602 \cdot 10^{-19} C$
Reduced Planck's constant	$\hbar$	$1.055 \cdot 10^{-34} Js$
Hartree energy	H	$4.360 \cdot 10^{-18} J$
Coulomb's constant	k_c	$8.988 \cdot 10^{9} Nm^2/C^2$

Table D.1: Atomic units and their SI values

In the simulations we work with atomic units. The parameters are given in

units of energy and time. The relevant energy scale here is electron Volt (eV). The relevant time scale of the laser pulses is in the order of picoseconds (ps). [1]

$$E_h = 27.2\ eV, \tag{D.1}$$

$$t_0 = \frac{\hbar}{\mathrm{E_h}} \approx 2.4 \cdot 10^{-5}\mathrm{ps}. \tag{D.2}$$

Examples:
The coupling constant: $g = 100\ \mu\mathrm{eV} = 3.67{\cdot}10^{-6}$ a.u.
The standard deviation of the gauss-shaped laser pulse: $\sigma = 35$ ps $= 1.46{\cdot}10^{6}$ a.u.

In the literature, quantities like the coupling constant or the scattering rates are often given in units of a frequency (Hz). The relationship is given by

$$\nu = \frac{E}{\hbar 2\pi}. \tag{D.3}$$

For example: $g = 76\ \mu\mathrm{eV} \mathrel{\widehat{=}} 18.4$ GHz

[1] In addition we use: $1\ \mathrm{eV} = 1.602 \cdot 10^{-19}$ J, $\hbar = h/(2\pi)$, $h = 6.626 \cdot 10^{-34}$ Js

Danksagung

Zunächst möchte ich mich bei meiner Familie bedanken, die mir während des gesamten Studiums helfend zur Seite stand. Insbesondere richtet sich mein Dank an meine Mutter **Alberta**, die mich immer mit offenen Armen empfängt und mein Elternhaus zu einem Zuhause macht. Danke für den Rückhalt den du mir gibst. Meinem Vater **Wilhelm** danke ich für das Interesse an der Natur und ihren Wundern, welches er schon früh in mir weckte. Den vielen Gesprächen mit dir und den zahllosen Wanderungen, die immer auch Lehrgänge waren, verdanke ich die frühe Schulung im wissenschaftlichen Denken und die Freude am Verständnis der Welt.
Mit meinem Betreuer **Ulrich Hohenester** hatte ich das Glück von einem großartigen Physiker und Menschen lernen zu dürfen. Danke für deine Geduld und die Tür die immer offen stand.
Meinen Freunden und Kollegen, die mich durch das Studium begleitet haben, möchte ich für die vielen gemeinsamen Erlebnisse, die lustigen Erinnerungen und die innigen Freundschaften danken.
Besonderer Dank gebührt den zwei Männern an meiner Seite. Meinem Sohn **Jakob**, der es wie kein anderer versteht meine Aufmerksamkeit, nach einem langen Uni-Tag, wieder auf die wirklich wichtigen Dingen zu lenken und **Andreas**, für die Motivation, den Glauben an meine Fähigkeiten und deine Liebe.

Bibliography

[1] Lucio Claudio Andreani, Giovanna Panzarini, and Jean-Michael Gerard. Strong-coupling regime for quantum boxes in pillar microcavities: Theory. *Physical Review B*, 60:13276 – 13279, 1999.

[2] K. Bergmann, H. Theuer, and B. W. Shore. Coherent population transfer among quantum states of atoms and molecules. *Reviews of Modern Physics*, 70:1003–1025, 1998.

[3] Heinz-Peter Breuer and Francesco Petruccione. *The theory of open quantum systems*. Oxford University Press, 2002.

[4] Tapash Chakraborty. *Quantum Dots*. Elsevier Science B.V., 1999.

[5] U. Gaubatz, P. Rudecki, S. Schiemann, and K. Bergmann. Population transfer between molecular vibrotional levels by stimulated raman scattering with partially overlapping laserfields. a new concept and experimental results. *Journal of Chemical Physics*, 92:5363–5375, 1990.

[6] K. Hennessy, A. Badolato, M. Winger, D. Gerace, M. Atatüre, S. Gulde, S. Fält, E. Hu, and A. Imamoglu. Quantum nature of a strongly coupled single quantum dot-cavity system. *Nature Publishing Group*, 445:896–899, 2007.

[7] Ruth Houbertz, Jochen Schulz, Jesper Serbin, and Boris N Chichkov. Schnelle Herstellung photonischer Kristalle. *Physik in unserer Zeit*, 36:278–285, 2005.

[8] G. Khitrova, H.M. Gibbs, M. Kira, Koch S.W., and Scherer. Vacuum rabi splitting in semiconductors. *Nature physics*, 2:81–90, 2006.

[9] Michael A. Nielsen and Isaac L. Chuang. *Quantum Computation and Quantum Information*. Cambridge University Press, 2000.

[10] Preskill. *Quantum Information and Computation*. available online at http://www.theory.caltech.edu/people/preskill/ph229, 1998.

[11] William H. Press, Saul A. Teukolsky, William T. Vetterling, and Brian P. Flannery. *Numerical Recipes*. Cambridge University Press, 2007.

[12] Marlan O. Scully and M. Suhail Zubairy. *Quantum Optics*. Cambridge University Press, 1997.

[13] H. Shull and G.G. Hall. Atomic units. *Nature*, 184:1559, 1959.

[14] Wolfgang Stumpf. Quantenpunkte als Photonenquellen. *Physik in unserer Zeit*, 39:71–76, 2008.

[15] Kerry J. Vahala. Optical microcavities. *Nature*, 424:839–846, 2003.

[16] Nikolay V. Vitanov, Thomas Halfmann, Bruce W. Shore, and Bergmann Klaas. Laser-induced population transfer by adiabatic passage techniques. *Annual Review of Physical Chemistry*, pages 763–809, 2001.

[17] D. F. Walls and Gerard J. Milburn. *Quantum Optics*. Springer, 2008.